Online Journal of Space Communication

Volume 3
Issue 6 *Satellite Security (Winter 2004)*

Article 6

June 2021

International Guidelines for the Preservation of Space as a Unique Resource

Phillip D. Anz-Meador

International Guidelines for the Preservation of Space as a Unique Resource

Phillip D. Anz-Meador, Ph.D.
Embry-Riddle Aeronautical University
Dept. of Physics

Abstract

Introduction

The non-benign nature of spaceflight had been recognized well before the first on-board sensors detected the van Allen radiation belts about the Earth or piezoelectric sensors, meant to measure strain and flexure within the structure of a rocket or spacecraft, first noted the impacts of micrometeoroids on the craft (*Explorer 1*, Alexander, personal comm.). Indeed, the recognition that meteoroids were "burning" in the upper atmosphere implied the requirement of a source of particles to burn, hence the studies of both photographic and radar/radio meteors. Observations of the sun, as well as such terrestrial phenomena as the Aurora Borealis and Australis, and such celestial phenomena as comets, asteroids, and the faint reflection provided by the meteoroid complex (the so-called "Zodiacal light"), provided further evidence, if needed, as to the significant constituents (and potential hazards) in the space environment.

Means of protecting spacecraft from this natural environment were required, and a significant amount of laboratory and on-orbit testing was conducted in order to protect and preserve spacecraft functions. Almost all measures were passive in nature, *e.g*. shielding was deployed to protect electronics from cosmic rays and micrometeoroids, designs were optimized to prevent static discharge, and "rad-hard" (radiation hardened) electronics were developed to cope with the ambient radiation environment. Time passed, and space became a place to explore, to do business, and to protect global security.

During that time, an appreciation of the many and varied components of the space environment grew. A large body of literature developed to characterize, explain, and predict the effect of the ambient environment upon spacecraft and space materials. It is not the intent of this paper to review that portion of the environment.

The near static nature of some of the components was noted, as well as the dynamic nature of others. Yet this was not the only categorization possible. For example, some (notably Mr. John Gabbard) noticed oddities in the catalogs of space objects tracked by the North American Aerospace Defense Command (NORADCOM). Certainly it wasn't common knowledge that not only had we launched the LANDSAT 1 spacecraft aboard a Delta rocket, but evidently hundreds of other small objects with this launch. Further analysis indicated that

these objects were debris associated with the accidental fragmentation of the Delta's second stage. Again, time passed. Military tests were conducted in space, including intentional explosions and collisions, and the list of accidental explosions grew.

Debris began to accumulate and, with a maturity of thought not present at the dawn of the Space Age, scientists and engineers in the United States came to realize that spacecraft must not only be protected from the "natural" environment on-orbit, but also the induced, or "man-made" environment. Finally, a burgeoning sense of environmental stewardship led to the modern international consensus that not only must spacecraft be protected from their environment, but that same environment must be protected from spacecraft.

This, then, is the subject of this paper: what is being done to protect spacecraft from the macroparticle (to include both anthropogenic debris and meteoroids) environment, and what is being done to protect the environment from man's presence. Only a holistic view of these processes can ensure a future environment safe for its navigation and capable of sustaining continued growth and exploitation of the unique natural resource offered us by space. Thus, in this paper we shall review the international guidelines being formulated to protect both spacecraft and the environment. To place these in context for the general reader, we shall start by providing an overview of the current space environment and environmental effects upon spacecraft.

Environmental Overview

The man-made space environment

The man-made component of the overall space environment is usually categorized into five types of objects, and as well by the object's active or inactive status. The five types are spacecraft or payloads, rocket bodies or rocket boosters, operational debris, fragmentation debris, and anomalous debris. To be more explicit, we may define the types as follows:

- Spacecraft or payloads: active or inactive (in storage, or derelict) vehicles or objects whose purpose was the primary goal of their respective launch. While the term "spacecraft" is usually reserved for relatively complex vehicles, the broader term "payloads" describes all levels of sophistication, including such inert objects as calibration spheres and dipoles.

- Rocket bodies (or boosters; usually abbreviated as "R/B"): these vehicles provide the means of launch, orbital transfer, and orbital insertion to the payloads. Thrust is provided by liquid fuel engines, solid fuel motors, or gaseous and/or electric/ionic thrusters. Size ranges from over ten meters in length (*e.g*. the Commonwealth of Independent State's [CIS] *Zenit*, or SL-16 [US Dept. of Defense designation], R/B) to small ullage motors

used to settle liquid propellants and ejected by the CIS *Proton*'s (SL-12) fourth stage.

- Operational debris: debris released during stage separation, payload deployment, or payload operations. These may include, respectively, straps and bolts; adapters, clamp bands, and spin/de-spin weights ("yo" weights); and retention or hold-down straps and radiator or sensor covers.

- Fragmentation debris: debris created during the planned or accidental explosion of, or collision between, payloads and/or R/B. Though not cataloged due to their size, debris produced by collisions of small objects with large targets could logically fit into this category.

- Anomalous debris: debris created by unknown means, usually long after payload deployment or end-of-mission. While the majority of instances have produced one or two anomalous objects, some (such as the Cosmic Background Explorer [COBE] or the SNAPSHOT nuclear reactor-powered test satellite). It has been suggested (Johnson, N., personal comm.) that while fragmentation debris are a measure of space traffic's effect upon the environment, anomalous debris *may* be a measure of the environment's effect upon resident space objects.

The approximate distribution of objects by type is depicted in Fig. 1; the reader should note that these objects are exclusively 10 cm (approximately) and larger in size, and are cataloged using ground-based sensors.

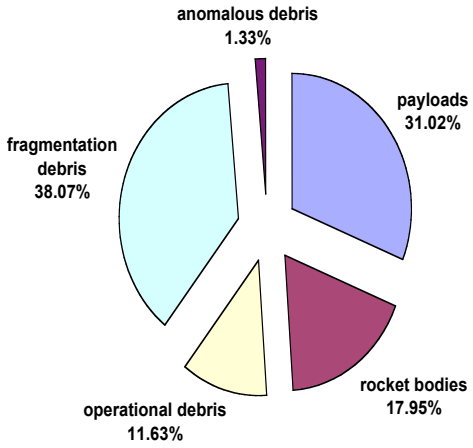

Fig. 1. Objects by type.

In addition to those debris objects produced as a satellite undergoes a fragmentation, debris have been identified as belonging to solid rocket motor (SRM) exhaust compounds (Al_2O_3) and paint pigments (surface degradation products). In the case of Aluminum Oxides, the *Explorer 46* meteoroid survey satellite observed, with 95% confidence, a correlation between SRM firings and an increase in the incident, directional flux within 20 days of the firing//7//. Such time-sequenced

events may have been observed by the Long Duration Exposure Facility's Interplanetary Dust Experiment//8// and the SkiYMET meteor radars (Ref. X3) as well. Both exhaust products and paint pigments have been identified by scanning electron microscopy and elemental analysis in impact crater residue. Human biological wastes have also been identified by this technique//9//, though these particulates should normally be confined to altitudes below about 400 km, the maximum altitude of most manned missions.

Degradation debris have also been measured on-orbit. Also referred to as local contamination, these debris tend to be most prevalent during the first weeks or months of operations; as such, they are similar to "out gassing" effects (Ref. X2).

Once classified by general type, a second objective method of characterizing the man-made population is by size and mass. The following table (after Ref. X4, with updated information) portrays the gross distribution of resident space objects in size and mass.

SIZE [cm]	NUMBER OF OBJECTS	% NUMBER	% MASS
0.1 – 1.0	35,000,000	99.67	0.035
1.0 – 10.0	110,000	0.31	0.035
> 10.0	8000	0.02	99.93
TOTAL:	35,118,000	100.0	1,400,000 kg

Table I. A statistical breakdown of the on-orbit man-made population. The total percent mass represents that fraction of a total estimated mass loading of 1,400,000 kg; this figure is based upon the NASA space traffic model and the Dept. of Defense Space Control Center (SCC) catalog.

The categorization by size is not coincidentally broken out in decades of size; objects greater than approximately 10 cm (in low Earth orbit, or LEO) are observed by ground-based sensors, tracked and correlated, and cataloged by agencies performing the space surveillance mission worldwide. Those between 1 and 10 cm may be observed by special radars during statistical data collection campaigns, while those smaller are rarely observed. Rather, objects smaller than 1 mm are typically assessed by counting the number of impact features on surfaces exposed to, and returned from, space.

Yet another means of characterizing the environment is by the spatial density S, *i.e*. the number of equivalent objects per cubic kilometer. This quantity, derived in a manner analogous to that in the classical theory of gasses, is of great utility as it may be related to both the flux F and the expected collision rate C:

$$F = S \cdot v \text{ [impacts/m}^2\text{/year]}$$

and

$$C = F \cdot A = S \cdot v \cdot A \text{ [impacts/year]},$$

where v is the relative velocity between an object (the “target”) and the impactor (the “projectile”) and A is the area (cross-sectional or surface area) of the target object. The incident flux represents the number of particles striking a surface within a given time; the flux is usually expressed in units of [impacts/m^2/yr], but may appear in other units. An excellent analogue for the flux is the amount of water falling on the windshield of a vehicle driving through a rainstorm. The final amount will depend upon the size of the raindrops, or the distribution in size, the velocity of the drops, and the velocity of the vehicle as it drives through the storm.

The following figures (after Ref. X5) depict the spatial density of cataloged (> 10 cm in LEO, > approximately 1 m in Geosynchronous Earth orbit, or GEO) objects in LEO and deep space. The reader may mentally multiply the LEO figures by a factor of 300, and the GEO figure by a factor of 50, to obtain the flux at these altitudes.

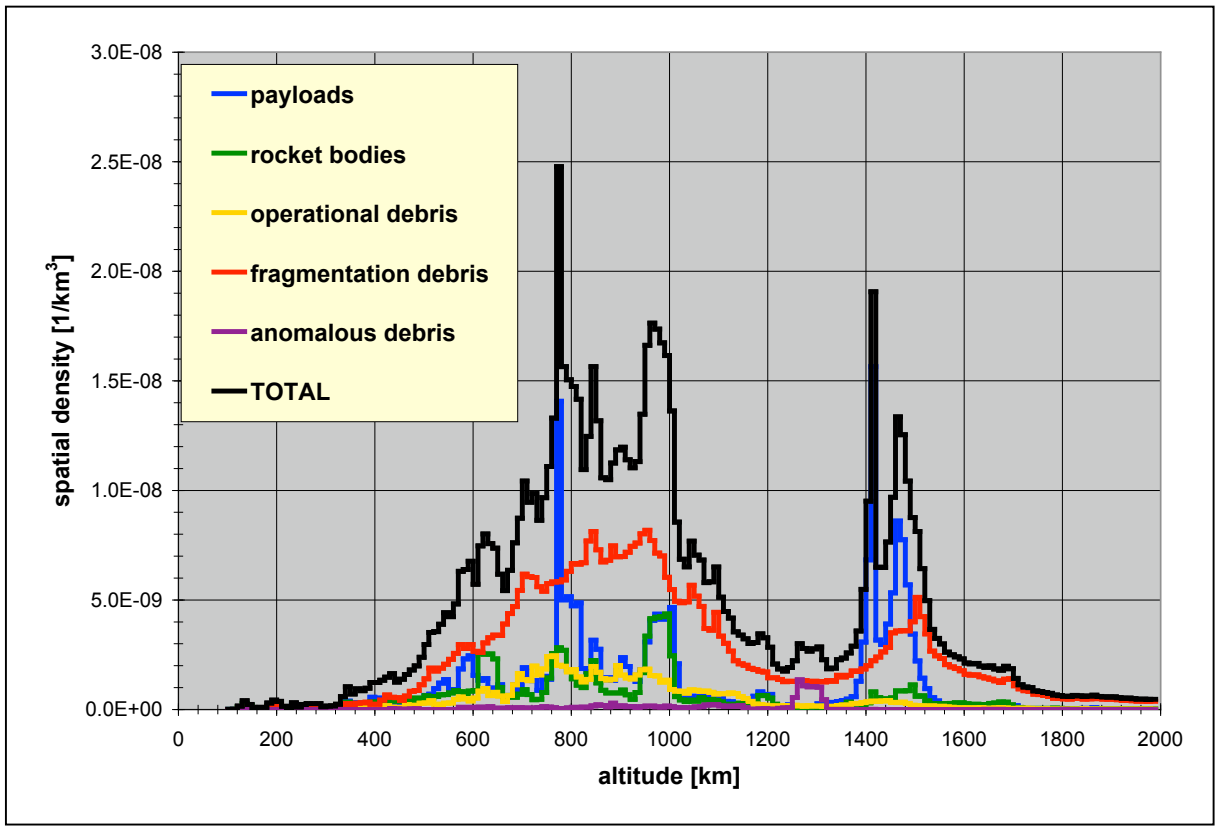

Fig. 2. The spatial density of equivalent satellite objects in LEO. Altitude divided into 10 km wide altitude bins. Spatial density portrayed on a linear vertical axis to emphasize altitudes of high absolute concentration.

In Figure 2, perhaps the most prominent features are the “spikes” event just below 800 km altitude, and just above 1400 km altitude. These result from the relatively dense packing of specific spacecraft in the Iridium and Globalstar commercial communication satellite constellations, respectively.

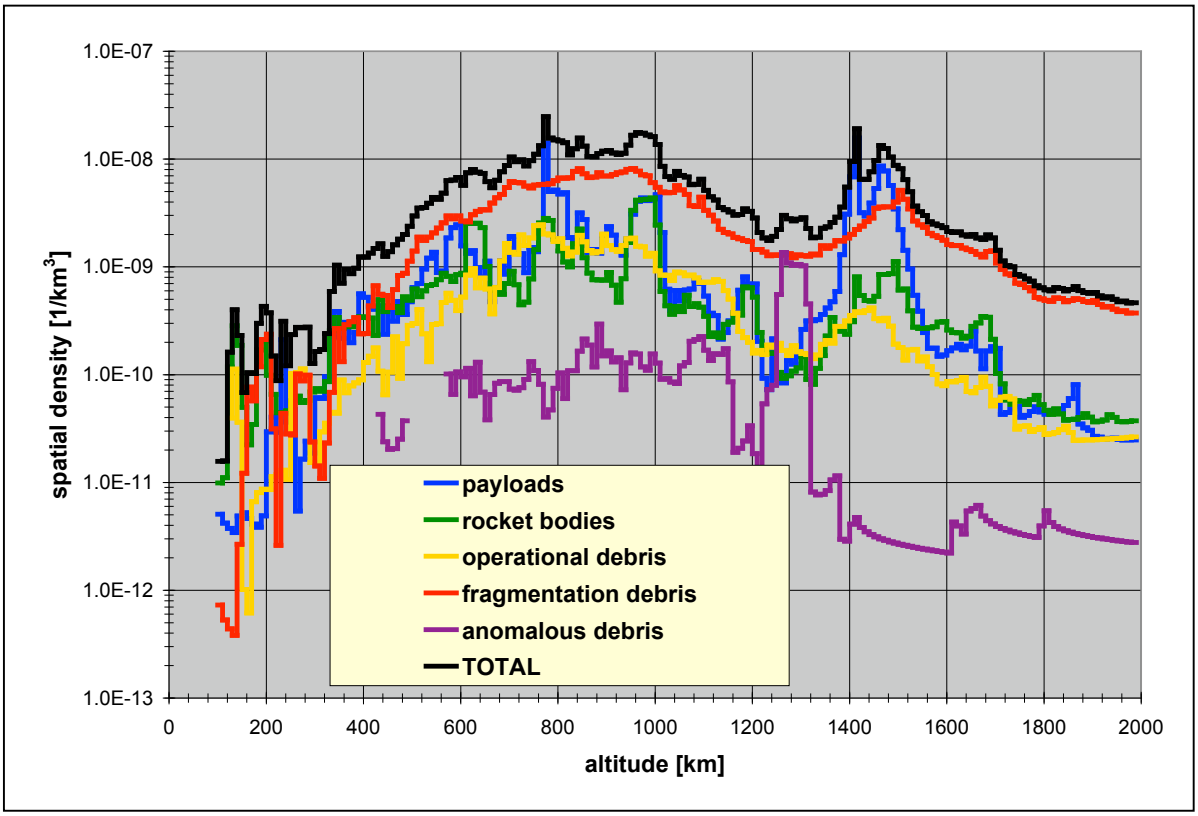

Fig. 3. The spatial density of equivalent satellite objects in LEO. Altitude divided into 10 km wide altitude bins. Spatial density portrayed on a logarithmic vertical axis to emphasize distribution by type, altitude, and concentration. Concentration of anomalous debris around 1300 km altitude due to the SNAPSHOT satellite.

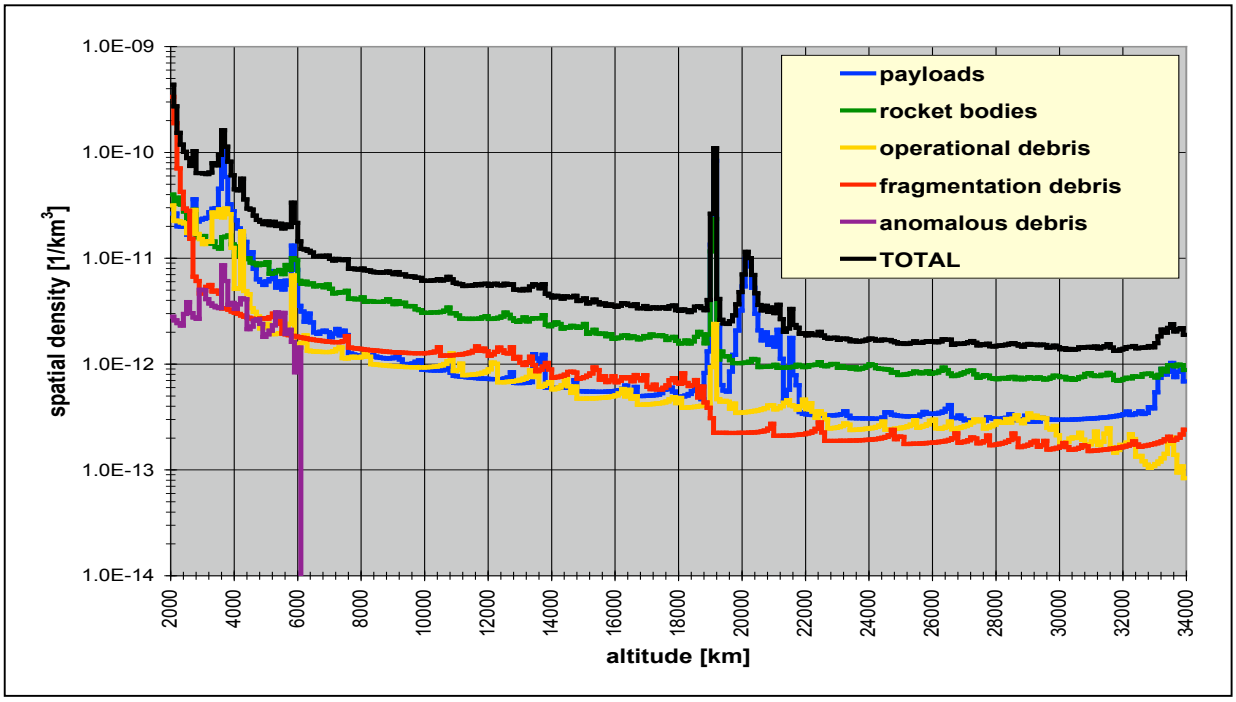

Fig. 4. The spatial density of equivalent objects in deep space (here, defined as altitudes above LEO and below GEO). Altitude in 100 km bins. Readily evident are the US and Russian navigation satellite constellations in middle Earth orbit.

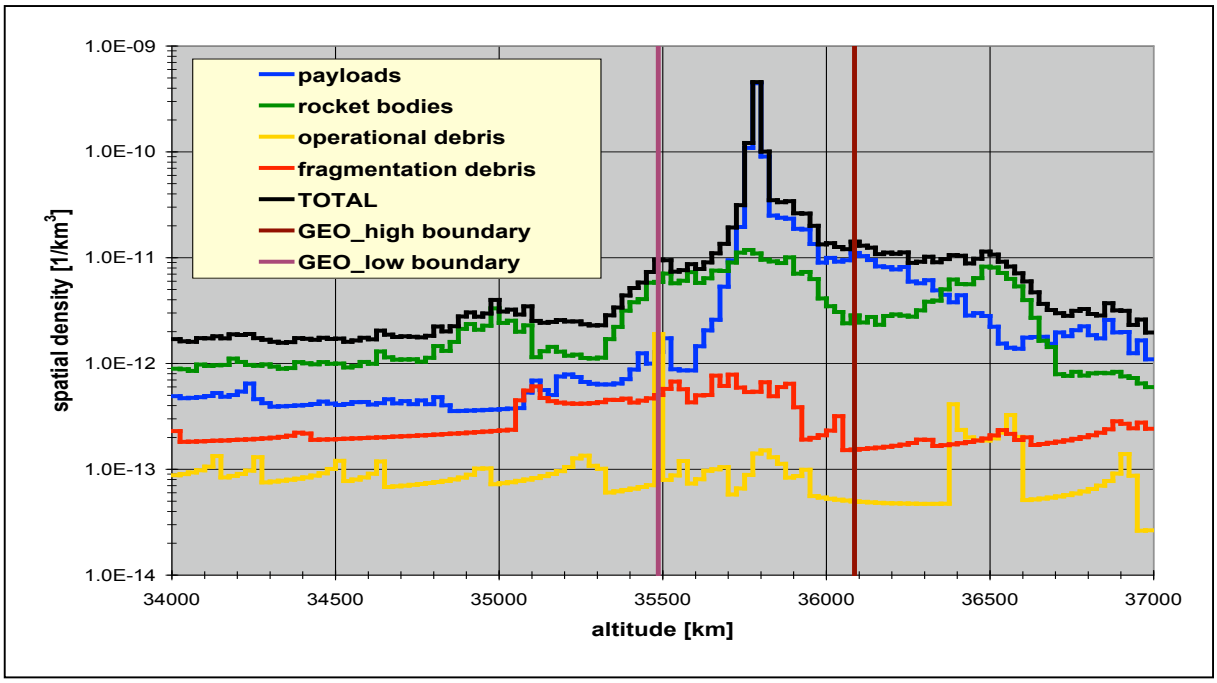

Fig. 5. The spatial density of equivalent objects near GEO. Altitude in 100 km bins. “High” and “Low” boundaries define a nominal GEO operational region.

Because these figures only portray those objects capable of being cataloged (with certain exclusions for national security), it is important to recall that these are larger than approximately 10 cm in LEO and larger than 1 m in GEO. Whereas the LEO region is believed to be reasonably complete, this is not the case in deep space, and GEO in particular. Recent measurements (Ref. X6) indicate that a significant population of objects larger than 10 cm reside in the GEO belt. One reason for this may lie in a historical undercounting of objects (primarily operational debris) released in the GEO belt. For example, objects such as solar array retention straps have not been cataloged for many historical payloads. Unrecognized fragmentations may also have contributed to the GEO local environment. Thus, the GEO environment portrayed in Fig. 5 may substantially be undercounting the actual spatial density/flux.

While these charts depict the distribution of cataloged objects, they are not directly translatable to either a “high quality” flux or a collision rate. In the case of a flux, this is because the relative velocity between two objects depends on the actual orbital properties of the pair of objects involved in any prospective collision. For objects whose orbital planes are randomly distributed with respect to each other and the remainder of the population, these are:

- the apogee (maximum altitude) and perigee (minimum altitude) of each object in the pair; and
- the inclination (the angle between the orbit plane and the Earth’s equator) of each object.

Apogee/perigee altitudes determine the velocity, as a function of altitude, of each of the individual objects. For circular orbits, as are the majority in LEO, MEO, and GEO, the orbital velocities of both objects are roughly equal, and collisions on the front and sides surfaces of the “target” object are prevalent. However, if one object is in an elliptical orbit (*i.e*. a large difference in perigee and apogee altitudes), then (a) the elliptical orbit, at perigee, may be traveling up to 3 km/s faster than the other object, and (b) the object in the elliptical orbit may therefore “catch up” with the other object and strike it from “behind”. This is observed on-orbit, as shuttles and other spacecraft flying at 28° inclinations commonly return with a multitude on craters on their rearward-oriented surfaces. The inclination is also an important determinant of the outcome of any collision, as certain inclination allow for “head on” collisions at up to 14-15 km/s. Conversely, the uniformly low inclinations found in GEO, along with the coordinated motion of the objects there, tends to lower the relative velocities possible.

Another factor contributing to the calculation of collision rate is the relative cross-sectional area of projectiles and targets. While Figures 2 and 3 indicate two roughly equivalent peaks in spatial density at around 800-1000 km and 1400-1500 km altitude, more collisions are expected to take place at the lower altitude. This is because the objects resident at and about that altitude are significantly larger (many being derelict SL-16 R/B), and hence present more “target area”,

than are the spacecraft around 1400-1500 km altitude. This has been confirmed by high fidelity long-term computer modeling of the evolution of the environment.

Computer models, based on measurements of the environment (including the analysis of objects returned from space), are used to project an "average" environment due to objects smaller than those depicted in Figures 2-5.

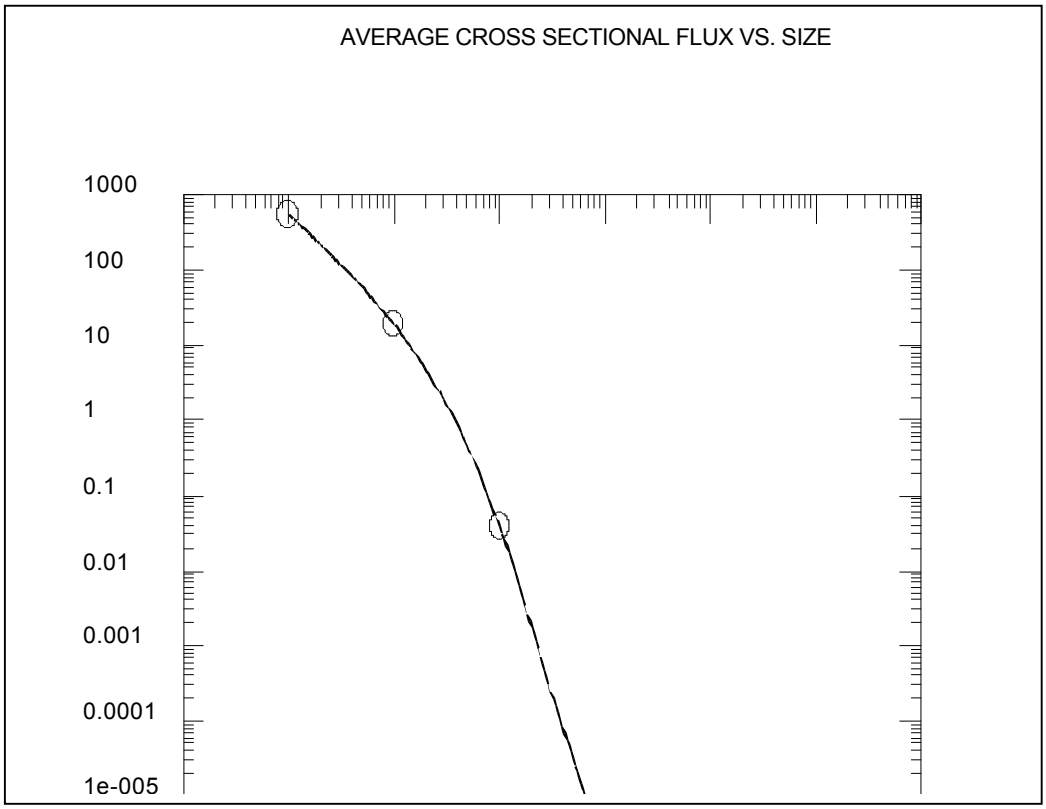

Fig. 6: The modeled environment for 1 □m-1 m impactors; target orbit is 400 km circular, 51.6° inclination (similar to the ISS nominal orbit).

Figure 6 depicts the output of the NASA ORDEM2000 computer model (Ref. X7). As may be seen, the cumulative flux due to the debris population 1 mm and larger in size is five (5) orders of magnitude larger than the cataloged population.

Effects upon spacecraft

As of this writing (November 2003), there has been only one (1) recognized accidental collision between cataloged objects: the French *Cerise* satellite's gravity gradient stabilization boom was cut by a piece of French debris produced by the 1986 fragmentation of an *Ariane* R/B third stage. All other historical (alleged) collisions were conducted as military anti-satellite or ballistic missile defense tests. The vast majority of fragmentations have been accidental explosions.

These explosions range in severity from mission survivable (*e.g*. a battery box explosion aboard the NOAA 8 spacecraft) to the catastrophic, in which a body is totally destroyed in the blast. Therefore, this section will concentrate on the effects of impacts on spacecraft.

A qualitative assessment of impact effects is provided in the following table, after Ref. X1.

DIAMETER OF IMPACTOR [cm]	EFFECT
< 0.01	Surface erosion
< 0.1	Potentially serious damage to spacecraft
0.3 at 10 km/s relative velocity (typical in low Earth orbit)	Equivalent to being struck by a bowling ball traveling at 60 mph (88 ft/s)
1.0 at 10 km/s relative velocity	Equivalent to being struck by a 400 lb safe traveling at 60 mph

Table II. Effects of particles of a given size upon spacecraft surfaces.

It is illustrative in a quantitative sense to examine the dependency of the probability of impact or penetration upon environmental and physical variables. Environmental variables are those dependent upon the orbital characteristics of the target (and projectile) objects, such as the relative velocity between the two; physical variables include the mass densities of the materials constituting the two objects.

The effect of the incident flux may be characterized by the Poisson probability of one or more ($n \geq 1$) impacts of size 'd' and larger is:

$$P_{n\geq 1}(d) = 1 - e^{-\int\int \mathbf{F} \bullet d\mathbf{A} \cdot dv},$$

where $\mathbf{F}(d,v)$ is the size and velocity-dependent flux, $d\mathbf{A}$ is the differential unit of surface area, n is the number of impacts, and integrals are performed over both surface area and the velocity distribution.

A common figure of merit for estimating the hazard to spacecraft (for example, in calculations performed for the International Space Station [ISS] and the space shuttle fleet) is the probability of no penetration, or PNP. The PNP may be expressed using the Poisson statistic $P_0 = \exp(-N)$, where:

$$N \propto v^{\alpha} \cdot \phi(v) \cdot T^{\beta} \cdot (\cos\theta)^{\gamma} \cdot \rho_t^{\delta} \cdot \rho_p^{\varepsilon} \cdot A \cdot t \ .$$

The variable T is the surface thickness, θ is the impact angle measured from surface normal, v is the relative velocity, $\phi(v)$ is the fraction of velocities between v and v + dv, ρ is a mass density, A is the area of the exposed surface, and t is

the elapsed time of exposure. The subscripts 't' and 'p' refer to target and projectile, respectively, and the set (□,□,□,□,□) are, in general, non-integer rational numbers. Additional dependencies relating to target yield and tensile strengths//12// or other material characteristics//13// may be manifest. Multi-layer shielding and body self-shielding can modify these relations.

Impacts in MEO and GEO occur at correspondingly lower velocities. However, even in GEO, the average relative velocity is on the order of 500 m/s, with a maximum around 1.5 km/s. As such, and to apply a terrestrial measure, these are commensurate with being struck by either "standard" or "high velocity" ammunition.

While the debris population accounts for roughly half of all objects tracked and cataloged by the US, simple calculations reveal that the impact rate of these cataloged objects onto a one m^2 target, per year, is minuscule. However, small untracked debris do present a meaningful hazard to spacecraft because of accelerated aging of spacecraft components, degradation of sensitive surfaces such as mirrors, optical surfaces, radiators, and solar panels, and the potential for a 'mission kill' should a single-point failure mode be susceptible to impact by small debris. The STS-50 mission provides an example of component degradation//4//, as segments of the radiator assembly were required to be replaced following approximately 10 days of flight with the payload bay facing in the direction of the velocity vector (the so-called "ram" direction). Shuttle flight deck windows are also replace with a frequency of (on average) one outer pane per mission. High pressure propellant lines, pressurized storage vessels, and exposed cable bundles provide additional examples of single-point failure mode elements on small spacecraft.

An Orbital Debris Bibliography

Since a paper of this nature cannot review all aspects of the orbital debris hazard, the reader is referred to Appendix A. This appendix consists of a bibliography of salient papers and books discussing man-made debris and the space environment.

International Activities to Preserve the Space Environment

The preceding discussion summarizes the current (2003) understanding of the man-made orbital debris environment. This understanding forms the basis of the international consensus regarding the space environment, and the reader is referred to Ref. X7A for a chronology of the development of that consensus within the US government and its efforts in the commercial and international space communities. This "consciousness raising", begun at NASA Johnson Space Center (JSC) in the late 1970s, has today led to an international consensus among the international space agencies, intergovernmental

organizations (*e.g*. the European Meteorological Satellite organization, EuMetSat), and non-governmental organizations (NGOs, *e.g*. INTELSAT).

The year 1993 was a watershed year for orbital debris studies. In April of that year, representatives of the major space faring powers met in Darmstadt, Germany, in order to formalize a working agreement and terms of reference for the interchange of technical information on orbital debris; this group formed the basis of the Inter-Agency Space Debris Coordination Committee (IADC). The current structure of the IADC is presented in Figure 7.

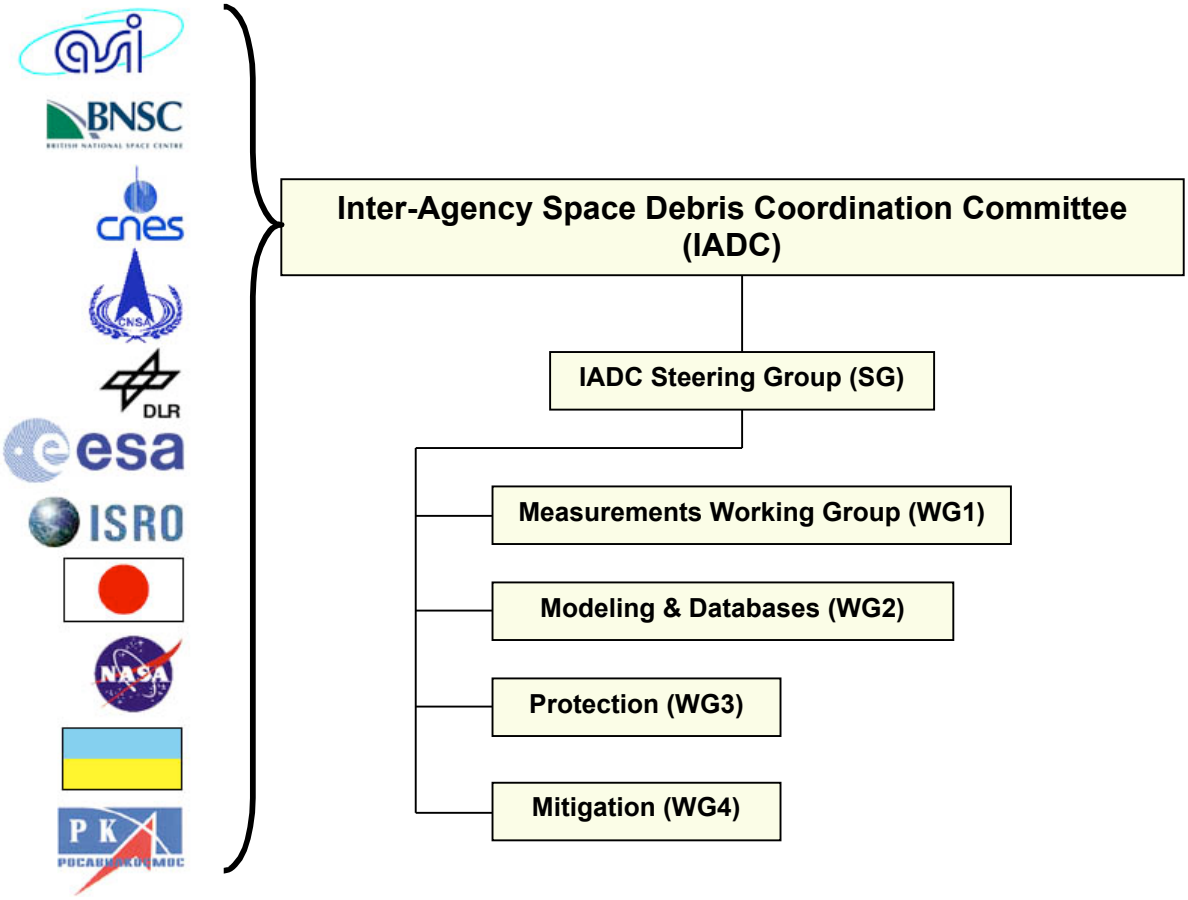

Fig. 7: IADC member and component structure.

Current members include ASI (Italy), the British National Space Centre (BNSC, UK), CNES (France), the Chinese National Space Agency (CNSA, People's Republic of China), the German Aerospace Center (DLR), the European Space Agency (ESA), the Indian Space Research Organization (ISRO), Japan, NASA, the National Space Agency of Ukraine (NSAU), and Rosaviakosmos (RKA of the CIS). The NASA delegation incorporates NASA, DoD, Federal Aviation Administration (FAA), and other US Government agency activities. Canada and Brazil have enjoyed observer status at recent meetings of the IADC.

In June 1993, a meeting on orbital debris was held at the United Nations (UN). At this meeting, the subject of orbital debris was introduced onto the agenda of the UN's Committee for the Peaceful Uses of Outer Space (COPUOS) Science & Technology Subcommittee (STSC). The UN COPUOS has become a valued partner to the IADC's activities and in 2004 will begin monitoring several voluntary debris-reduction compliance activities of the IADC's member agencies.

In response to an increased awareness of the hazards posed spacecraft operations by the orbital debris environment, as well as the environmental impact of accidental and intentional explosions, collisions, and other events depositing materials into the environment, the international space agencies have begun to codify their requirements on the manufacturers and owner/operators. Specifically, these requirements have taken the form of national (or otherwise "local") handbooks of regulations. While these are generally similar in scope and content, it is useful to review their general construction and requirements prior to the activities of the IADC.

Regulatory Activities

Technological Activities

Under the auspices of the IADC, the general program of debris-related activities has coalesced around four major activities. These are measurement of the environment, modeling, protection, and mitigation. The first two activities are focused on assessing the current environment and enabling the user community to make reasonable projections into the future. This is essential, as it allows trade studies to be made of various protection and mitigation strategies. Protection activities are oriented towards protecting the spacecraft from the environment, whereas mitigation activities are dedicated efforts to protect the environment from the man-made orbital population. Each activity is discussed in detail below.

Measurement

Measurement activities are of fundamental importance to characterizing the current environment, as well as monitoring the environment over time in order to assess either growth or, ideally, a reduction in the number of particles in the environment. There are two primary methods by which the environment is measured: ground-based (and recently, space-based) remote sensing and *in situ* measurements. The latter may be divided into those materials which have been returned from orbit and analyzed in the laboratory for their serendipitous information content, and dedicated flights of impact sensors.

Ground- and space-based remote sensing of the environment requires a substantial national investment in the means. Historically, space surveillance was driven by the need to distinguish a ballistic missile attack from the population of Earth orbital objects during the Cold War for early warning, cueing anti-ballistic missile (ABM) systems, and impact point prediction. For that reason, only the United States and Soviet Union (and its successor, the Commonwealth of Independent States) have fielded comprehensive space surveillance systems and networks. These are discussed at length in Appendix B in terms of sensors, capabilities, data reduction, data products, and their general availability.

The space surveillance networks are limited in many ways. For example, the geographical distribution of sensors provided both limitations in surveillance and opportunities for unobserved maneuvers and other on-orbit operations to be conducted. For our purposes, however, the physics of the sensors involved was the primary limiting factors as to their usefulness. In low Earth orbit, the smallest observable object is generally considered to be on the order of 10 cm (4 inches) in size. Unfortunately, the most statistically likely impactors are well below that size. Select sensors can measure the environment to smaller sizes (in the case of the US' Long Range Imaging Radar [LRIR] in Massachusetts, down to about 5 mm). Indeed, a significant amount of information on the small particle environment has been collected by the LRIR and the co-located NASA/DoD Haystack Auxiliary (HAX) radar, as well as the German FGAN [*q.v.*] and others. These data have been essential in the formulation of modern engineering models of the space environment in LEO. However, these sensors are limited in terms of field of view, resource allocation, and budget. Hence, the need to develop other means of sensing the small particle environment.

The USSR and its follow-on states have flown micrometeoroid (and inclusively, debris) experiments aboard the "Nauka" piggyback scientific modules of the so-called third generation photo-reconnaissance *Cosmos*-series satellites. These data led to the development of the Soviet-era □OCT (GOST, or State Planning Commission) model, which contained three components: sporadic "background" meteoroids, meteoroid streams/showers, and what were assessed to be meteoroids in Earth orbit. This latter population is, rather, indicative of man-made clouds of orbital debris. Witness plates (passive plates of various materials which provide information via the cratering record on their surfaces) have also been flown aboard the *Salyut* (USSR/France) series and *Mir* (France/NASA, Ref. X8,X9,X10) space stations.

Early US measurements of the environment were oriented exclusively towards meteoroids, as might be expected, given the relatively insignificant human traffic at that time. *Explorer I*, the first American satellite, carried piezoelectric microphones and wire grid detectors which recorded the impacts of small solid particles. *Explorer XIII, XVI, XXIII* and *46* were dedicated missions to measure the micrometeoroid environment using a variety of sensor technologies. *Pegasus 1-3*, the instrumented Saturn IV third stages of several *Apollo*

boilerplate models, also measured micrometeoroid (and most likely debris) impacts upon large extensible panels. From these measurements, as well as those of sensors mounted about Lunar and interplanetary probes, models of the sporadic micrometeoroid environment were developed. Ground-based photographic and radar observations of meteors formed the primary data source for models of the stream meteoroid environment. The meteoroid portion of the space environment is considered to be relatively well characterized by computer models at this time. These are useful in discriminating meteoroids from orbital debris.

Modern *in-situ* measurements of the solid particle environment have concentrated upon the analysis of materials returned from space. These measurement's debris component is isolated by subtracting meteoroid impacts from the total impact record. This may be accomplished in a statistical sense using the meteoroid environment models described previously or in a deterministic sense by scanning electron microscopy and element analysis of the residue found in the impact crater. Typically, meteoroid craters possess element compositions quite different from those caused by man-made orbital debris. Materials from the Long Duration Exposure Facility (LDEF), the European Recoverable Carrier (EURECA), the Solar Maximum Mission (SMM), *Westar 6*, and *Palapa B* have all contributed to an understanding of the environment; SMM and LDEF have been the primary and most analyzed sources. With the exception of the mildly elliptical orbits of the stranded Westar and Palapa communication satellites, however, all analyzed surfaces were exposed at or below approximately 500 km altitude. No consistent, long-term *in-situ* measurements of the environment above 500 km altitude (including both the remainder of LEO and the GEO belt) have been made.

However, recent progress in measuring the small particle environment has been made with the US' ARGOS satellite (elliptical orbit) and the European Space Agency's GORID sensor (GEO).

Modeling and characterization

Protection

The protection of a space asset may take the form of either passive or active means. Passive means are those performed during the design process and typically incorporate either dedicated shielding, or the placement of internal and external components in such a manner as to benefit from collateral shielding by adjacent components.

Passive Spacecraft Shielding

Active Collision Avoidance

At the present time, several important US national and international assets are continuously monitored for collision avoidance (COLA) maneuver planning purposes. Most prominent are the manned National Space Transportation System (STS, the "Space Shuttle") and the International Space Station (ISS). The USSTRATCOM is the responsible agency for these activities, and in fact maintains a dedicated workstation capability for this activity. COLA activities utilize SP element sets [*q.v.*] and a projection period of three (3) days to provide a long-range forecast of close approaches, or conjunctions. Should a conjunction be predicted, USSTRATCOM notifies NASA JSC Mission Control/Mission Operations Directorate (MOD) and maneuver planning is implemented. The following sections describe current best practice in planning activities related to maneuvering the STS and ISS.

National Space Transportation System (STS)

The US STS orbiter vehicle (OV) was the first space vehicle to institute active collision avoidance practices. This practice is predicated upon the penetration of a volume or volumes centered on the position of the STS OV by an RSO.

Candidate collision objects (represented by their TLEs) are initially screened by apogee/perigee to determine if they would be capable of colliding with STS under any circumstances; for example, objects in circular orbit at 1450 km altitude were excluded at this stage, since they could never interact with the much lower STS orbit. Objects predicted to enter or cross the volume would draw attention to these objects, resulting in increased tasking of the SSN sensors to obtain better, more timely element sets, and the processing of these sets using USSPACECOM special perturbations (numerical integration) orbit propagator models. If the object continued to be predicted to enter the volume, the SSN would notify NASA so as to initiate planning for a collision avoidance maneuver. Between 1989, when the procedure was implemented, and February 1994, four such notifications were received and the STS maneuvered three times. This discrepancy in number is due to the manner in which the maneuver planning was implemented: maneuvers would be conducted only if such a maneuver doesn't compromise either the primary payload or mission objectives, which remains a qualitative decision on the part of STS management. In those cases involving a maneuver, the STS required approximately 45 minutes to plan and perform the maneuver.

The STS has historically used tiered threat ellipsoids (up to the mid-1990s) and later "boxes" (mid-1990s to 2000) arranged about, and centered on, the nominal position of the STS orbiter vehicle. Boxes (parallelepipeds) replaced ellipsoids due to their easier mathematical implementation and manipulation for COLA calculations. The introduction of boxes also coincided with the introduction of the concepts of an "alert" box and a "conjunction" box, the latter also being referred

to as the “coffin”. The coffin’s dimensions replicated the dimensions of the previous threat ellipsoid, *i.e*. 10 km (down-track) x 4 km (radial) x 4 km (cross-track). The alert box doubled these dimensions. Extensive analyses conducted at NASA JSC and supported by the USSTRATCOM have recently (2000) promoted a revision to the dimensions of the boxes. Currently, the dimensions of the conjunction box are 14 km x 14 km (cross-track and down track directions) x 2 km (radial direction). The alert box has expanded to dimensions of 40 x 40 km (down-track and cross-track) x 10 km (radial direction). Due to the “squashed” nature of this box, it is sometimes referred to colloquially as a “pizza box”, after the flat boxes used for home delivery pizza.

The STS orbit determination software did not generate variance/covariance information. Thus, STS conjunction predictions remained “deterministic” in the sense that any predicted conjunction, *i.e*. a penetration of the pizza box, signaled that a maneuver should be planned and a maneuvering burn by the on-board Orbital Maneuvering System (OMS) be performed. Modern collision avoidance analyses have indicated that this strategy is ineffective in calculating the true probability of collision. For example, the interaction of the collision box and the uncertainty in position of space debris objects did not correctly portray the geometrical relationship between these volumes and the evolution of the positional uncertainty over time. For this reason, the STS has recently adopted (Foster, personal comm., 2001) a methodology derived originally for the International Space Station (ISS).

International Space Station (ISS)

The ISS has adopted a more modern computational strategy by incorporating a mature implementation of time-varying ISS and space debris uncertainty estimates. The positions of objects are described in terms of state vectors, variance/covariance matrices, and propagation over time using special perturbation element set data and propagation software. This process tends to reduce the number of potential conjunctions as compared to previous strategies. At the current time, the ISS utilizes a single pizza box with dimensions of 40 x 40 km (down-track and cross-track directions) x 10 km (radial direction) as a single, alert box. Should an object penetrate this box and possess a probability of collision of 10^{-4} or greater, maneuver planning shall be implemented.

If a maneuver is possible (given time-acceleration constraints), the ISS will maneuver to evade the predicted conjunction. Mission success criteria have not influenced ISS maneuver strategy, as it has the STS, due to the ISS being in the construction phase. However, reduction of maneuvers to four of less per year, assuming the maneuvers to occur approximately every 90 days such that microgravity experiments may reasonably be expected to come to fruition before a maneuver is executed, has long been a programmatic goal. Therefore, mission success criteria may become important to the decision-making process in the future.

Remediation

The Legal Regime

Conclusions

References

1. Anonymous, "Meteoroid Environment Model-1969 [Near Earth to Lunar Surface]". NASA SP-8013 (1969).
2. Anonymous, Natural Environment for Space Station Design, Revision A. NASA SSP-30425/A (June 1989).
3. Reynolds, R.C., G.W. Ojakangas, and P.D. Anz-Meador, "Defining Orbital Debris Environmental Conditions for Spacecraft Vulnerability Assessment". J. Spacecraft Rockets **29**, no 1 (January-February 1992): 57-63.
4. Christiansen, E.L. *et al*., "Assessment of High Velocity Impacts on Exposed Space Shuttle Surfaces". In Proceedings of the First European Conference on Orbital Debris, W. Flury *ed*. (Darmstadt, Germany: ESA SD-01, 1998): 447-52.
5. Anz-Meador, P.D. and A.E. Potter, "Density and Mass Distributions of Orbital Debris". Paper IAA-94-IAA.6.4.689, presented at the 46th Congress of the International Astronautical Federation, Jerusalem, Israel, 9-14 October 1994.
6. Reinhardt, A., W^{m} Borer, and K. Yates, "Long Term Orbital Debris Environment Sensitivity to Spacecraft Breakup Parameters" **DRAFT**. Presented at the World Space Congress, Washington, D.C., September 1992.
7. Kessler, D.J., "Impacts on Explorer 46 from an Earth Orbiting Population". In Orbital Debris, D.J. Kessler and S.-Y. Su, eds., NASA CP-2360 (1985): 220-32.
8. Oliver, J.P. *et al*., "Estimation of Debris Cloud Temporal Characteristics and Orbital Elements". Adv. Space Res. **13**, no. 8 (August 1993): 103-6.
9. Bernhard, R.P., and D.S. McKay, "Micrometer-sized Impact Craters on the Solar Maximum Satellite: The Hazards of Secondary Ejecta". In Lunar

and Planetary Science XIX, Part 1 (Houston: Lunar and Planetary Institute, 1988): 65-6.

10. Stansbery, E.G., D.J. Kessler, T.E. Tracy, M.J. Matney, and J.F. Stanley, "Haystack Radar Measurements of the Orbital Debris Environment", NASA JSC-26655 (20 May 1994).

11 Anz-Meador, P.D., "A Model of the Thermal and Electrical Properties of Cosmic Dust Particles". Ph.D. dissertation, Baylor University, Waco, Texas, 1989.

12. Watts, A.J., and D. Atkinson, "Dimensional Scaling for Impact Cratering and Perforation". Presented at the 3rd LDEF Post-Retrieval Symposium, Williamsburg, VA, 1993.

13. McDonnell, J.A.M., and K. Sullivan, "Hypervelocity Impacts on Space Detectors: Decoding the Projectile Parameters". In Hypervelocity Impacts in Space, J.A.M. McDonnell, ed. (Canterbury, UK: University of Kent Press

X1. Interagency Group (SPACE), for the National Security Council, "Report on Orbital Debris", Washington, D.C., February 1989.

X2. Galicia, G.E., B.D. Green, M.T. Boies *et al*., "Particle Environment Surrounding the Midcourse Space Experiment Spacecraft". J. Spacecraft Rockets **36**, no. 4 (July-August 1999): 561 ff.

X3. Dushek, O., W.K. Hocking, and N. Mitchell, "Investigation of the Possible Detection of Earth-Orbiting Particulates by SKiYMET Meteor Radars". Can. Undergrad. Phys. J. **1**, no. 2 (January 2003): 7-11.

X4. Office of Science & Technology Policy, "Interagency Report on Orbital Debris". Washington, D.C., November 1995.

X5. Anz-Meador, P.D., History of On-Orbit Satellite Fragmentations, 12th ed. NASA JSC-29517, Houston, Texas, USA. 31 July 2001.

X6. Flury, W., A. Massart, T. Schildknecht *et al*., "Searching for Small Debris in the Geostationary Ring – Discoveries with the Zeiss 1-metre Telescope". ESA Bulletin no. 104 (November 2000): 92 ff.

X7. Liou, J.-C., M.J. Matney, P.D. Anz-Meador *et al*., "The New NASA Orbital Debris Engineering Model ORDEM2000". NASA TP 2002-210780, Houston, Texas, USA. May 2002.

X7A. Portree, D.S.F. and J.P. Loftus Jr., Orbital Debris and Near-Earth Environmental Management: A Chronology. NASA Ref. Pub. (RP) 1320, December 1993.

X8. Hörz, F., G. Cress, M. Zolensky, T.H. See, R.P. Bernhard, and J.L. Warren, "Optical Analysis of Impact Features in Aerogel From the Orbital Debris Collection Experiment on the *Mir* Station", NASA/TM-1999-209372, August 1999.

X9. Mandeville, J.C., "Cosmic Dust and Orbital Debris: Collection on MIR Space Station", Adv. Space Res. **11**, no. 12 (1991): (12)93-(12)96.

X10. Mandeville, J.C., and L. Berthoud, "Hypervelocity Impacts on Space retrieved Surfaces: LDEF and MIR". In Hypervelocity Impacts in Space, *ed*. J.A.M. McDonnell (Canterbury, UK: U. of Kent at Canterbury, 1991): 196-199.

Appendix A

An Orbital Debris Bibliography

Appendix B

Space Situational Awareness *via* Space Surveillance

World Space Surveillance Systems

United States of America

The US space surveillance system is the US Strategic Command's (USSTRATCOM) Space Surveillance Network (SSN). The SSN is a global network of radar and electro-optical surveillance sensors and gives the USSTRATCOM the ability to detect, track, identify and catalog all man-made resident space objects (RSOs) down to a threshold size. The USSTRATCOM is a unified command within the US military, *i.e*. it is composed of (US) Air Force Space Command (AFSPC), the Naval Space Command (NAVSPACECOM), the (US) Army Space Command (USARSPACE), and other contingents, including a Canadian contingent under the auspices of US-Canadian agreements related to defense of the North American continent. The principal components of the SSN are depicted in the following wire diagram.

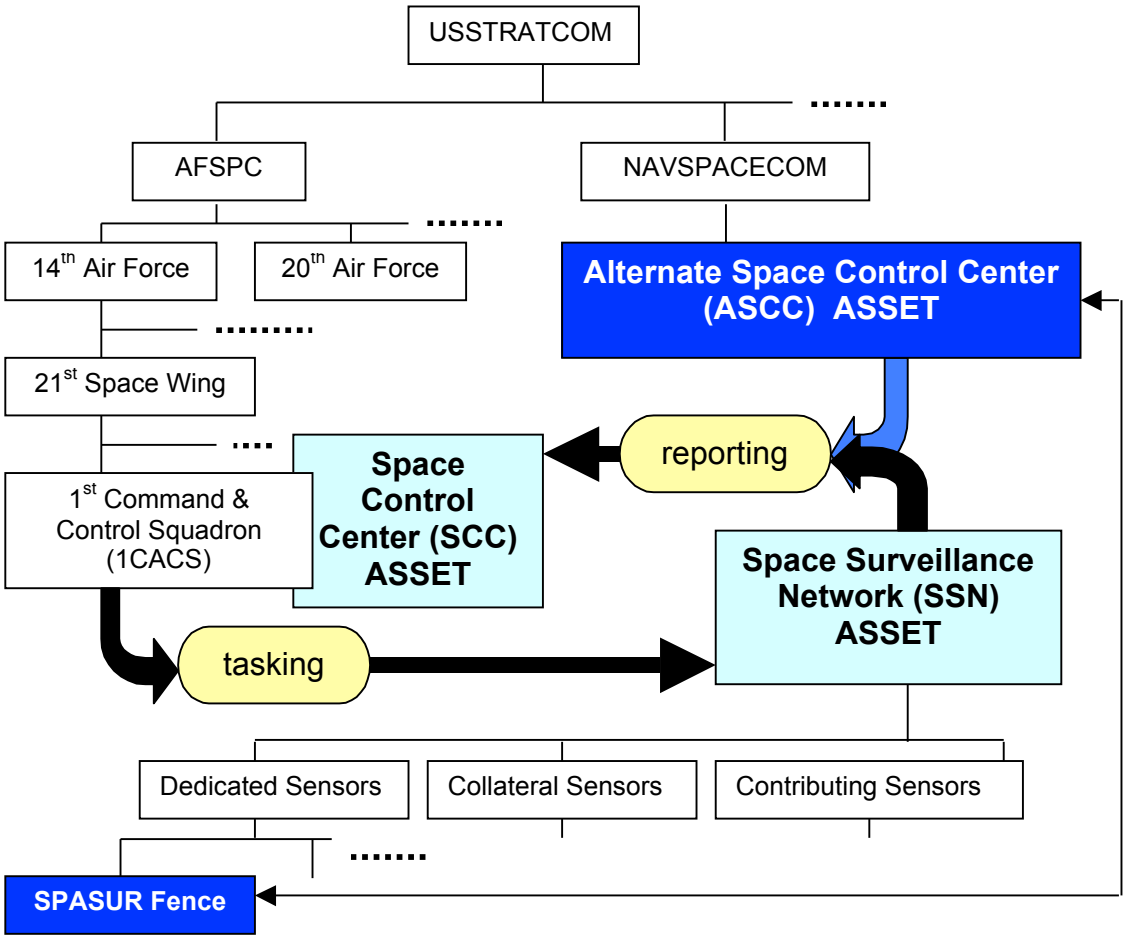

The Space Control Center (SCC) and the 1st Command & Control Squadron (1CACS) are co-located in Colorado Springs, Colorado, USA, as indicated by being contained in the dotted box at left. The Alternate SCC is located at the Headquarters NAVSPACECOM in Dahlgren, Virginia, USA. The ASCC is a less robust version of the SCC, and may serve to off-load certain activities of the SCC during intensive periods of activity. Finally, the SSN itself is composed of dedicated sensors, collateral sensors, and contributing sensors. Dedicated sensors refer to those sensors controlled by USSTRATCOM and dedicated to the space surveillance rôle, *i.e*. direct SSN support. Collateral sensors are those controlled by USSTRATCOM but dedicated to other, non-SSN support activities. The contributing sensors are non-USSTRATCOM controlled sensors whose primary activity is not SSN support yet provide occasional support under contract or interagency agreement with USSTRATCOM. Dedicated sensors consist of those operated by NAVSPACECOM (the so-called Naval Space Surveillance [NAVSPASUR] SPASUR "fence") and by AFSPC (all remaining dedicated sensors). The SSN is detailed further in the table below.

Sensor	Sensor Desig.	Rng Type	Collector Type	Operating spectrum	Mission Support
Antigua	ANT	NE	Radar (Mechanical Tracker)	C band	Collateral
Ascension	ASC	NE	Radar (Mechanical Tracker)	C band	Collateral
Beale – PAVE PAWS	BLE	NE	Solid State Phased Array Radar (SSPAR)	UHF	Collateral
Cape Cod – PAVE PAWS	COD	NE	SSPAR	UHF	Collateral
Cavalier – PARCS	CAV	NE	Radar PA	UHF	Collateral
Clear – BMEWS	CLR	NE	3 Detection Radars & 1 Tracking Radar	UHF	Collateral
Diego Garcia - GEODSS	DGC	DS	E-O	Visible	Dedicated
Eglin	EGL	NE/DS	Radar PA	UHF	Dedicated
Fylingdales - BMEWS	FYL	NE	SSPAR	UHF	Collateral
GLOBUS II	GLO	NE/DS	Radar (Mechanical Tracker)	X band	Dedicated
Haystack Aux - LSSC	HAX	NE/DS	Radar (Mechanical Tracker)	K_u band	Contributing
Haystack LRIR - LSSC	HAY	NE/DS	Radar (Mechanical Tracker)	X band	Contributing
Kaena Point	KAE	NE	Radar (Mechanical Tracker)	C band	Collateral
Kwajalein – ALCOR	ALC	NE	Radar (Mechanical Tracker)	UHF	Contributing
Kwajalein – ALTAIR	ALT	NE/DS	Radar (Mechanical Tracker)	UHF/VHF	Contributing
Kwajalein – TRADEX	TRX	NE/DS	Radar (Mechanical Tracker)	L & S band	Contributing
Kwajalein – MMW	MMW	NE	Radar (Mechanical Tracker)	mm wave	Contributing
Maui – GEODSS	MAU	DS	E-O	Optical	Dedicated

Millstone – LSSC	MIL	NE/DS	Radar (Mechanical Tracker)	L band	Contributing
MSSS – 3.7m	AEOS	DS	E-O	Visible	Contributing
MSSS - 1.6m	AMS	DS	E-O	Visible, LWIR	Contributing
MSSS - 1.2m	MOT	DS	E-O	Visible, LWIR	Contributing
MSSS - .8m	BDT	DS	E-O	Visible	Contributing
MSX/SBV	MSX	NE/DS	E-O	Visible	Dedicated
NAVSPACECOM Detection Fence	NAV	NE/DS	Radar (Detection Fence/Interferometer)	CW UHF	Dedicated
Socorro – GEODSS	SOC	DS	E-O	Visible	Dedicated
Shemya	SHY	NE	Radar PA	L band	Contributing
Thule	THU	NE	SSPAR	UHF	Collateral

Herein, each sensor is described by name, three-letter designator, sensor range profile, sensor type, and sensor category. Sensor range is defined as either/or Near Earth (NE) or Deep Space (DS). Near Earth RSOs are those with periods of 225 minutes or less (corresponding to semimajor axis altitudes of approximately 5876 km or less) while DS RSOs are of course the remainder of the RSOs. In terms of sensor type, mechanical trackers are the classic "dish"-type radars which acquire and track objects by pointing and steering the dish. Phased array radars (PAR) utilize electromagnetic beam steering to sweep the sky, and thus can search a significantly greater volume of space as compared to the beam (colloquially termed a "pencil beam" to give some idea of its relative diameter to "length" dimensions) generated by a mechanically-steered radar. The "E-O" sensors are electro-optical telescopic sensors. Other pertinent acronyms are the Moron Optical Space Surveillance (MOSS) sensor, the Lincoln Space Surveillance Center (LSSC), Midcourse Science Experiment (MSX) Space-Based Visible (SBV) optical sensor, the Ground-based Electro-Optical Deep space Surveillance System (GEODSS), the Millimeter Wave (MMW) radar located at US Army Kwajalein Atoll (USAKA), the Maui (Hawaii) Space Surveillance Site (MSSS), the Perimeter Acquisition Radar Attack Characterization System (PARCS) PAR, and the various Ballistic Missile Early Warning Sites (BMEWS). Radar operating frequency bands are as tabulated below.

BAND DESIGNATION	FREQUENCY RANGE
Very High Frequency (VHF)	50-300 MHz
Ultra High Frequency (UHF)	300-1000 MHz
L	1-2 GHz
S	2-4 GHz
C	4-8 GHz
X	8-12 GHz
K_u	12-18 GHz
mm wave	40-100+ GHz

In general, the smallest object diameter “d” (or characteristic length, [m]) detectable by a given radar is on the order of:

$$d = \frac{c}{2\Delta f} ,$$

where “c” is the speed of light (~ 3 x 10^8 [m/s]) and f is the frequency [Hz] quoted in the table above. Note, however, that this is extremely dependent upon target characteristics (both physical and geometrical), sensor processing/noise threshold(s), target minimum range, *etc*. Deep space tracking relies primarily upon optical tracking, and as such is similarly dependent upon target albedo (or reflectivity) and other characteristics as above, phase function, *etc*. The relative efficiency of one type of sensor (radar or E-O) lies in the relative dependencies of “target signal returned to the sensor”, S, to range. In general,

$$S_{radar} \propto \frac{1}{r^4} , \quad S_{E-O} \propto \frac{1}{r^2} ,$$

where r is the range from sensor to target object. Because the signal strength returned drops off faster with range for radars than for E-O sensors, radars historically have predominated in NE data collection, while E-O sensors have collected the majority of DS data. Note, however, that several radars (*e.g*. Eglin, and the Haystack LRIR and Millstone radars) have traditionally deployed a significant DS capability.

The SSN is portrayed in the following figure. Coverage indicated is for objects at 800 km clearing the local (topocentric) sensor horizon. Blue indicates the coverage pattern of radar sensors while red indicates the coverage pattern of electro-optical sensors. Several points must be made here. Though both sensor types are patterned for 800 km orbits, the higher minimum elevation of the optical sensors reduces the effective maximum coverage area. Furthermore, the areas portrayed in this figure are, with the exception of PARs, the maximum coverage areas. Neither mechanically-steered radars or electro-optical sensors, both being bore-sighted instruments, can observe more than a tiny fraction of the depicted spatial volume at any one time. Only PARs, and the Naval interferometer fence, can survey the total areas indicated over the course of a few-second sweep time or instantaneously (in the case of the fence).

Several salient features are apparent in this figure. Firstly, the global nature of the SSN becomes apparent. Secondly, one notes that the electro-optical sensors (DS sensors) are located at latitudes closer to the equator than other sensor types; this is because telescopes offer better deep space performance than radars and the majority of DS objects are at low inclinations or in the Geosynchronous belt. Despite the global coverage, the paucity of NE sensors at low latitudes limits the detection probability of low inclination objects or objects in

DS transfer orbits. Tracking of objects in GTO and those RSOs subject to the so-called “Southern Perigee Anomaly” (highly elliptical orbits with perigees in the southern hemisphere) are difficulties arising as a consequence of this geographical distribution.

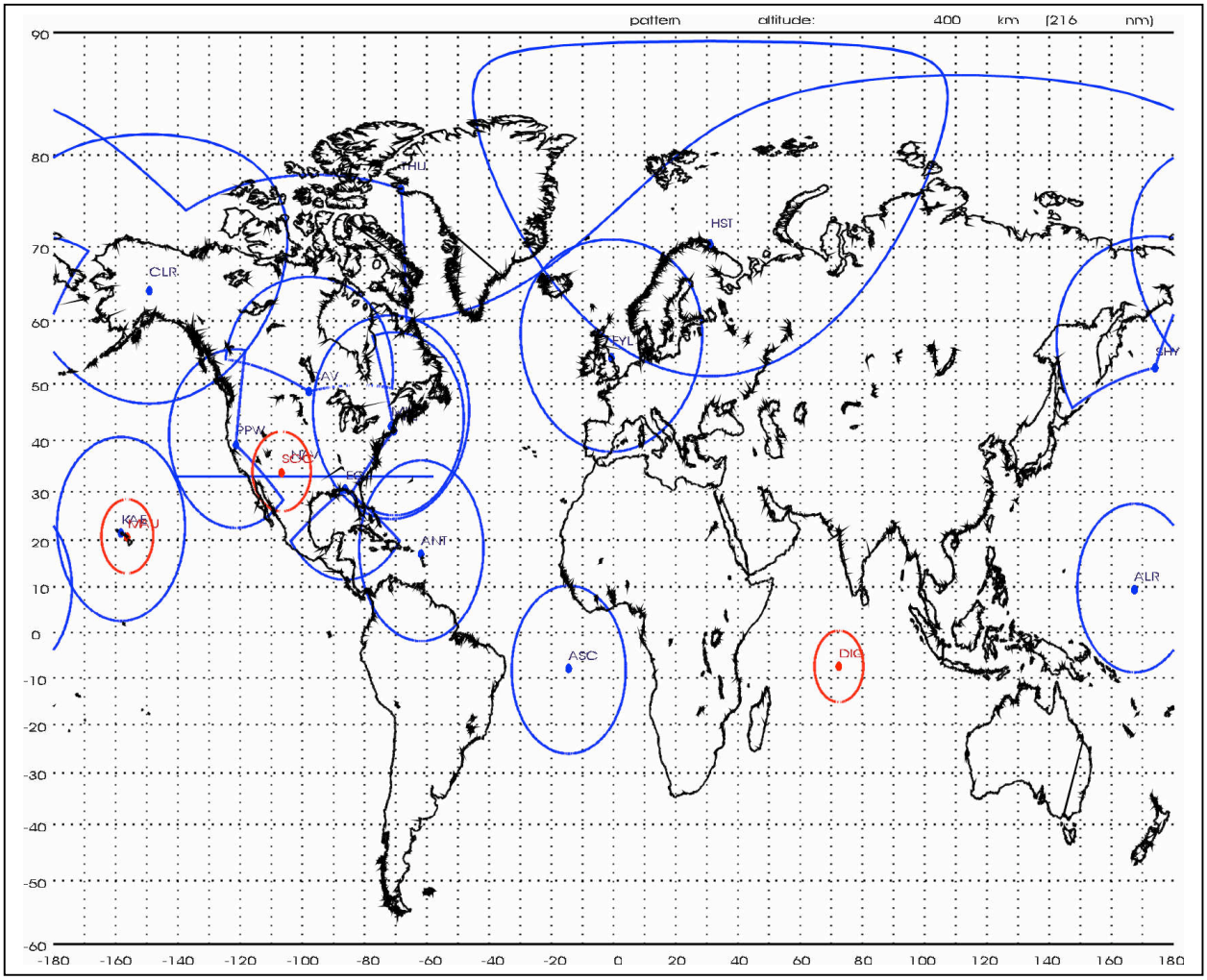

Fig. A-1: US SSN sensor assets.
Blue: RADAR sensor coverage at 800 km altitude; Red: E-O sensor coverage at 800 km altitude. See preceding text for discussion. Miller cylindrical projection.

One sensor is not portrayed here. The Midcourse Science Experiment (MSX) satellite’s Space-Based Visible (SBV) telescope is on orbit, and provides (primarily) Deep Space observations to the SCC. The MSX/SBV has proven the utility and flexibility of space-based optical space surveillance. This is important in terms of the potential decreasing available of foreign sites for ground-based sensors. As well, the SBV optical sensor is not subject to the vagaries of weather and the limited duty cycle of ground-based E-O sensors.

Data Processing

Numerical Processing

Two orbit determination and processing techniques are utilized by the USSTRATCOM. These may be referred to as General Perturbations (GP) and Special Perturbations (SP). USSTRATCOM also has other propagation routines on hand, *e.g*. the Semi-Analytic Liu Theory (SALT), and the reader should note that the Naval Space Command utilizes a different set of analytic, semi-analytic, and numerical integration-based orbit determination and propagation software.

GP processing utilizes the orbital dynamic theories of Kozai (Simplified GP model, or SGP) or Brouwer (SGP version 4, or SGP4), with modifications to include atmospheric drag, to perform orbit determination (including linear least squares differential correction) and element set generation. A proposed upgrade in the mid 1980s, utilizing the dynamic theory of Hoots (SGP version 8, or SGP8) was not proceeded with, though one will encounter references to it occasionally. Modifications to include third-body perturbations resulted in the Deep Space module for each propagator, *e.g*. SDP or SDP4. During processing, the Deep Space modules will be called should the period of the object(s) being propagated exceed 225 minutes. Backward compatibility with SGP/SDP has been maintained (see the discussion of element set format) because of computational limitations at many SSN sites as well as a large user community. At the present time, GP orbit determination within USSTRATCOM has been superseded by SP techniques *in toto*; GP remains in use, however, for creating the orbital elements sets issued by USSTRATCOM for public release.

SP processing is based upon numerical integration of the equations of motion, coupled with perturbation force models. Principal features of the SP processing may be summarized succinctly as follows:

- Geopotential: user-selected; usually smaller than 36x36, although capability to utilize higher fidelity is available
- Atmosphere: Jacchia-USSTRATCOM model with 10.7 cm Solar radio flux (F10.7) and Geomagnetic indices updated every six hours (in theory), though more likely every 24 hours (in practice), as the relevant databases are updated.
- Third-body perturbations: sun and moon, with a Geopotential smaller than 36x36.

Additional options, such as variable integration (time) step, are available. In practice, SP orbit determination requires that the users of SP data be informed as to every option utilized to process a particular observation, else the models used for orbit determination (USSTRATCOM) and propagation (the user) would differ. Within a given catalog, one may encounter two or more “different” SP models used, depending upon the circumstances of the differential correction

process applied (*e.g*. automatic *vs*. manual), the last update's epoch and sensor tasking priority, and other factors.

The Data Stream

As of a decade ago, the SSN was regularly processing over 50 000 observations per day; this load has increased, with existing sensors, over the course of the 1990s, and may be expected to increase further as (a) the on-orbit environment grows and (b) sensor capability upgrades decrease threshold detection sizes or extend observational capability to objects difficult to track with radar alone.

At the present time, approximately 80-90% of the catalog is updated using an automated differential correction process. For these objects, the updating is a near real-time process. The remainder require human intervention and are thus dependent upon manpower levels, tasking, priority, *etc*. Those objects failing this process are carried along as Uncorrelated Targets (UCTs) awaiting further confirmation in the form of additional observations by one or more sensors. In certain cases, objects have been discovered, or recovered after long periods of being lost, by the human analysis of long series of UCTs; twelve provisional fragmentation or anomalous events, one dating to December 1965, have been tentatively identified in this fashion in the last year. All were in difficult-to-track orbits (Geosynchronous transfer), possessed unusual physical characteristics, *e.g*. high ballistic/radiation pressure area-to-mass ratios, or both.

Not all state vector/element sets ("elsets") generated by the USSTRATCOM are transmitted to external sites, primarily the NASA Goddard Space Flight Center (GSFC) Orbital Information Group (OIG). Rather, those elsets determined to be "sufficiently different" from the preceding elsets only are transmitted. This operational technique was established to minimize traffic over what can only be considered antiquated transmission lines. Actual transmission criteria are a function of orbit type; there is no single criteria applied to the entire catalog. To cite specific examples, a low altitude and/or high-drag satellite will have more elsets transmitted per unit time than a relatively stable orbit of a satellite at 1500 km altitude. There is no relationship between the USSTRATCOM criteria for "attention" and "lost" objects and update criteria. However, if an elset is not updated within an internally specified time, tasking to the SSN sensors will be increased in an effort to update the object's orbital elements. If an elset has not been updated for 30 days, the object is considered "hard lost" and other techniques, *e.g*. NAVSPASUR fence searches and UCT processing, will be applied in an effort to reacquire the object.

The figure below presents a general outline of observation processing from initial observation to catalog entry update.

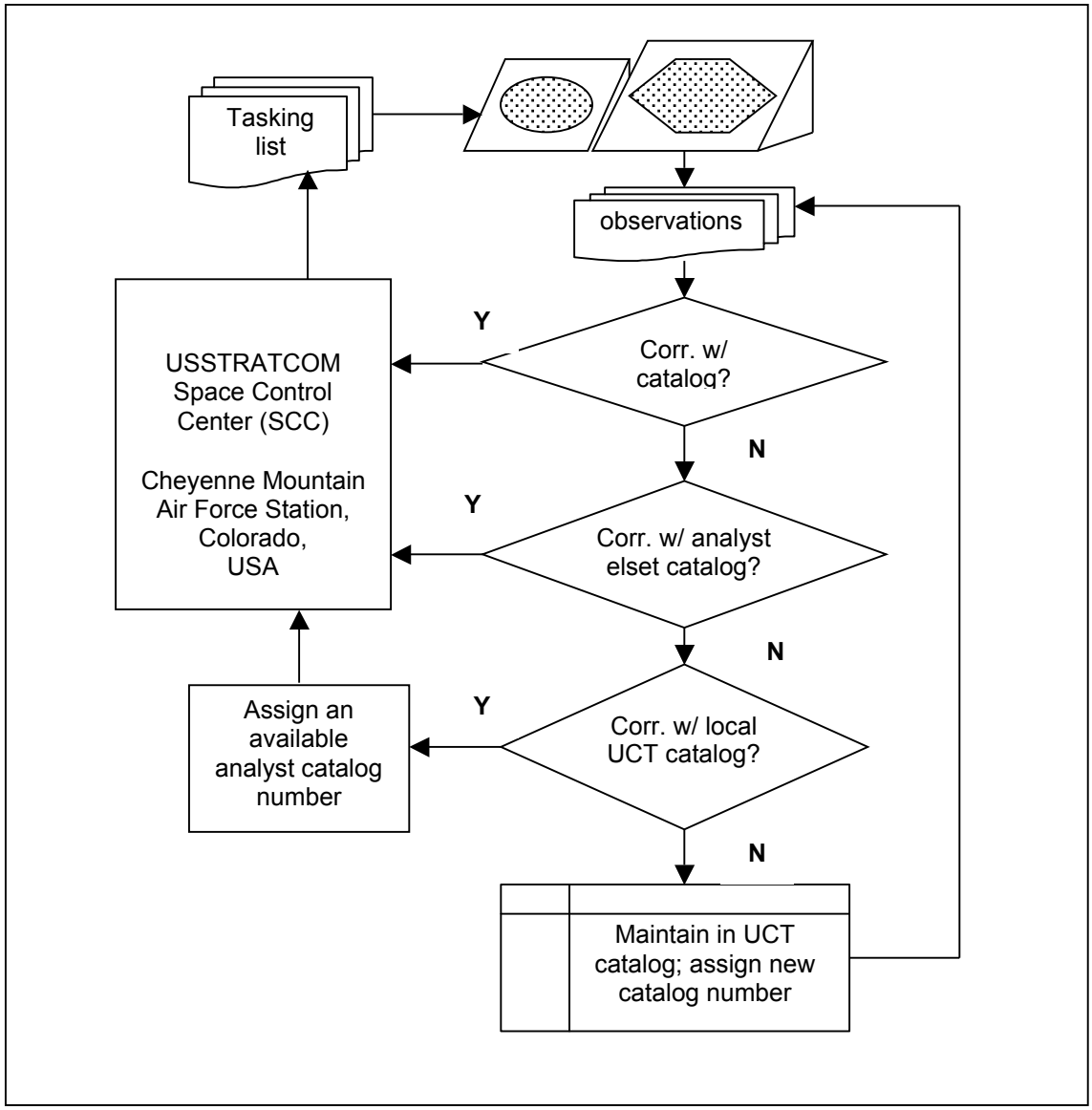

Fig. A-2: observational data evolution.

Automated orbit determination, track to track correlation, and cataloging activities account for updates to approximately 80-90% of the catalog at any given time. This process operates in near real-time. The remainder of the catalog require human intervention. This action may be necessitated by object maneuvers, high ballistic/radiation pressure area-to-mass ratios, or a breakup event. For these cases, hours to days may elapse before a quality state vector/element set can be built and distributed. Particularly in the case of fragmentation cataloging, the limitations imposed by the inherent quality of a given observation coupled with the need to correlate observations from track to track and avoid cross-tagging or other misidentification of the new object requires a significant effort on the part of

analysts. This task may be eased somewhat if the fragmenting body was in a unique or rarely utilized orbital regime (altitude or inclination) but is complicated for bodies in low inclination and/or high eccentricity orbits, or for orbits experiencing significant perturbations. For example, the fragmentation of the Long March 4 CBERS-1/SACI-1 rocket body in 2000 was a "clean" breakup (in analyst terminology) in that debris objects were well tracked initially, there was little opportunity for cross-tagging or misidentification, the event was at relatively low altitude, and other factors. Conversely, "dirty" breakups, such as the series of LANDSAT Delta rocket body fragmentations, are prone to cross-tagging and misidentification or misallocation to one of the three specific rocket bodies which fragmented. Several debris objects associated with these events have never entered the publicly available catalog. In certain cases, only long-term drag effects have rendered debris capable of entering the catalog; an example is provided by object 1961-015MM. This object, debris created during the 1961 fragmentation of this mission's Able-Star rocket body, only entered the catalog in the early 1990s.

Planned and Potential SSN Upgrades

Recent changes in the SSN have resulted in increased capabilities. Examples are provided by the recent (2000-2001) restoration of the Shemya-based *Cobra Dane* phased array radar to space surveillance activities and changes to Uncorrelated Target (UCT) processing at the AN/FPS-85 phased array radar at Eglin AFB. Optical sensors, such as those at the Maui Space Surveillance Site, also continue to be updated with new technology. Additional changes and upgrades to the SSN are expected to take place over the next two decades. Perhaps of primary interest would be the proposed upgrade of the Naval fence from UHF frequencies (~ 216 MHz) to a higher operating frequency; this would significantly improve this dedicated sensor's accuracy and ability to observe, track, and catalog smaller objects.

Data Format

Several formats are maintained by the SCC. These may be broadly defined as being of either a Cartesian state vector format or a Keplerian mean element set format. The latter includes the commonly encountered Two Line Element (TLE) set format, which will be described in detail.

Stave Vector (SV) Format

Two state vector formatted data produces are produced for special distribution by USSTRATCOM. The first is a (numerical) double precision state vector for a given satellite, generated using Special Perturbation (SP) theory, and the second is a satellite ephemeris for specified RSOs generated using either General Perturbation (GP) or SP theory.

The double precision state vector is defined as tabulated below. The reference frame is either Earth Centered Inertial (ECI) or Earth Fixed Greenwich (EFG).

ITEM	UNITS/COMMENTS
Satellite number	None
Epoch revolution	Revolution number at epoch/ascending node crossing
Epoch Time	(last two digits of year)(fractional day of year)
X position component	km
Y position component	km
Z position component	km
XDOT velocity component	km/s
YDOT velocity component	km/s
ZDOT velocity component	km/s
Bterm drag coefficient	m^2/kg (= $1/2C_DA/m$)

A second, larger "state vector" format is computed for special activities such as impact point prediction and combination of miss between orbits (COMBO) calculations. It is generated using SP processing and is essentially identical to the Satellite Ephemeris format. Satellite ephemeris data is defined below. Reference frames are either ECI or EFG. The (U,V,W) coordinate frame is defined such that the U axis is in the orbit radial direction, V is in the orbit down-track direction, and W is in the cross-track direction, or the direction of the orbital angular momentum vector.

ITEM	UNITS/COMMENTS
Date/time	Epoch time of ephemeris
Satellite number	None
Epoch revolution	Revolution number at epoch/ascending node crossing
Ephemeris type	"0" for data distributed outside of USSTRATCOM
Geodetic latitude LAT	Degrees
East longitude LONG(E)	Degrees
Altitude (HEIGHT)	km
Ground speed (VEL)	km/s
Heading (AZ)	degrees
Flight path angle (GAM)	degrees, measured with respect to local horizontal
Orbital Elements	
Semimajor axis (A)	km
Eccentricity (E)	none
Inclination (I)	degrees
Right ascension of ascending node	degrees
Argument of Perigee	degrees
True argument of latitude	degrees
Satellite Ephemeris	
X position component	km
Y position component	km
Z position component	km
XDOT velocity component	km/s
YDOT velocity component	km/s
ZDOT velocity component	km/s

Error Ellipsoid	
Semi-axis Magnitudes (3)	km
Spherical error (95% confidence)	None
U largest (U component of unit vector in the direction of the largest semi-axis)	None
U smallest (U component of unit vector in the direction of the smallest semi-axis)	None
U autre (U component of unit vector in the direction of the remaining semi-axis)	None
V largest (as defined above)	None
V smallest	None
V autre	None
W largest	None
W smallest	None
W autre	None
Position variance/covariance matrix	
σ_{UU}	None
σ_{UV}	None
σ_{UW}	None
σ_{VU}	None
σ_{VV}	None
σ_{VW}	None
σ_{WU}	None
σ_{WV}	None
σ_{WW}	None

Note that while the orbit determination software calculates the elements of the 3x3 variance/covariance matrix for both position and velocity, only the position matrix is available as a data product.

Element Set Format

Various multi-line element set formats have evolved over the course of the Space Age. These are described as being of “N lines” in format due to a heritage derived from IBM punch card data storage nomenclature. For example, the modern Two Line Element (TLE) set was originally stored on two punch cards; the “line” is the lineal descendent of an individual “card”. Thus, in certain older publications the reader will note references to “two card” or “three card” formats. The former is the ancestor of the modern TLE and is also referred to as the Transmission or T format. The latter is referred to as (USSTRATCOM) Internal or G format, and in fact four- and five-line formats exist and are processed and delivered to various customers. The format of the TLE set is tabulated below.

ITEM	FORMAT/ VALUES	UNITS
Satellite number	00001-69999	None
Classification	U	"U" indicates an Unclassified elset
International Designator	YYNNNAAA	(last two digits of year)(launch number within year)(alphabetic piece tag A-ZZZ)
Epoch Time	YYDDD.DDDDDDDD	(last two digits of year)(fractional day of year)
First derivative of mean motion with respect to time, divided by two (2)	±.NNNNNNNN	Revolutions/day^2
Second derivative of mean motion with respect to time, divided by six (6)	±(.)NNNNN±N	revolutions/day^3 (decimal place understood)
Drag coefficient B*	±(.)NNNNN±N	(Earth radii)$^{-1}$ (decimal place understood)
Ephemeris type	0	"0" indicates a TLE generated using the SGP4/SDP4 orbital model
Element number	NNNN	(usually) incremented every time an elset is updated
Check-sum (error checking)	N	None
Inclination *i*	NNN.NNNN	Degrees
Right Ascension of Ascending Node Ω	NNN.NNNN	Degrees
Eccentricity e	(.)NNNNNNN	None (decimal place understood)
Argument of Perigee ω	NNN.NNNN	Degrees
Mean Anomaly M	NNN.NNNN	Degrees
Mean Motion n	NN.NNNNNNNN	revolutions/day
Epoch revolution	NNNNN	Revolution number at epoch/ascending node crossing

A TLE set contains positional information for a given satellite and is currently transmitted as a General Perturbations (GP) element set ("elset"). In this elset format, the mean motion has been modified (referred to as being "Kozai'd") to be compatible with the Kozai Theory-based Simplified General Perturbations (SGP) astrodynamics model. The SGP4 model further modifies this format (*i.e*. de-Kozai's or un-Kozai's) to express the mean motion in its original Brouwer Theory form. The two theories of orbit propagation utilize two different pseudo-drag coefficients. In the case of SGP propagation, drag is characterized by a series expansion of the rate of change of the mean motion n over some time interval $\Delta t \equiv t_{i+1} - t_i$, viz:

$$n_{i+1} = n_i + \left(\frac{\dot{n}}{2}\right) \cdot \Delta t + \left(\frac{\ddot{n}}{6}\right) \cdot \Delta t^2 + \ldots$$

Due to the (relatively) frequent element set updating, the series expansion is truncated at the second derivative of n with respect to time. The coefficients of the Δt terms are contained in the TLE for SGP theory propagation. SGP4 propagation is effected using the pseudo-drag coefficient B* (pronounced "B

star"). This drag coefficient incorporates not only atmospheric drag, but indeed serves as a fit parameter in the orbit determination/update process. Therefore, this term may also incorporate effects due to sensor bias, unmodeled force terms (*e.g*. solar radiation pressure and atmospheric perturbations), variation in the drag coefficient C_D, RSO maneuvers, *etc*. B* [1/Earth radii] is theoretically related to the ballistic coefficient B [m^2/kg] and the RSO area-to-mass ratio (A/m) by the following equations:

$$B^* = \frac{\rho_0}{2} \cdot B$$

$$B = \frac{1}{2} \cdot C_D \cdot \frac{A}{m}$$

where ρ_0 is a constant atmospheric density equal to 2.461×10^{-5} [kg/m^2/Earth radii], C_D is the dimensionless drag coefficient, A is the cross-sectional area presented to the atmosphere [m^2], and m is the RSO mass [kg]. The drag coefficient of the "average RSO" is usually assumed to be on the order of 2.0 – 2.2. The reader is cautioned that difference publications define the ballistic coefficient in different manners, *i.e*. some include the factor of 1/2, some define B as the mass-to-area ratio, *etc*.

The epoch time is defined such that 0.00^h UT on 1 January of a given year (*i.e*. the midnight between 31 December and 1 January) is day-of-year 1.00000000, not 0.00000000, i.e. the elapsed time starts at 1 day rather than 0 days. Unlike the Julian day, TLE epoch times start at midnight UT rather than noon of a given day. Finally, TLE time is measured in mean solar days (1440 minutes duration) rather than sidereal days (1436 minutes duration). This can sometimes lead to confusion, as the SSC catalog (manifested as the publicly available monthly NASA GSFC OIG's "Satellite Situation Report") utilizes sidereal days.

The international designator is defined under United Nation conventions, and consists of a launch year, the numerical sequence of a given launch within the year, and an alphabetic piece tag. The piece tag is a character from A through Z, with the letters "I" and "O" omitted due to their possible confusion with the numerals 1 and 0 (zero), respectively. Piece tag "A" is usually assigned to the primary payload (or the first cataloged payload), "B" to a second payload or the rocket body, *etc*. The primary payload of the third launch of 2001 would therefore have an international designator of (20)01-003A. Should more than 24 pieces be associated with a given launch (for example, in the case of a fragmentation event), the piece tag is augmented by a second tag field. Thus, the 25^{th} and 27^{th} objects associated with this launch would be afforded international designators 2001-003AA and 2001-003AC, respectively. Should more than 600 pieces be generated (*i.e*. tags "A" through "ZZ" have been assigned), a third tag field would be added. Piece 601 would be assigned piece tag AAA, piece 604 would be assigned piece tag AAD, etc. A third field has been

necessitated only once, as over 700 trackable pieces were associated with the fragmentation of the STEP II rocket body, a Pegasus Hydrazine Auxiliary Propulsion Stage (HAPS). Prior to 1963, a Greek letter designator was applied in lieu of the launch sequence number, and a numerical identifier was applied in lieu of the alphabetic piece tag. Thus, 1961-015C is equivalent to 1961-□3 (omicron 3).

Commonwealth of Independent States (CIS)

The CIS (Russian) space surveillance network corresponding to the US SSN is the Russian Space Surveillance Service (RSSS), as usually referred to in the West, or the Outer Space Monitoring System (SKKP -- Sistema kontrolya kosmicheskogo prostranstva), to use its Russian title. The RSSS/SKKP is a subordinate command of the CIS Space Troops. Organization detail similar to that presented for the SSN isn't available for the RSSS. However, a general outline of the RSSS activity and cataloging process is possible based on publicly available data and presentations by RSSS representatives; this is presented in the following diagram.

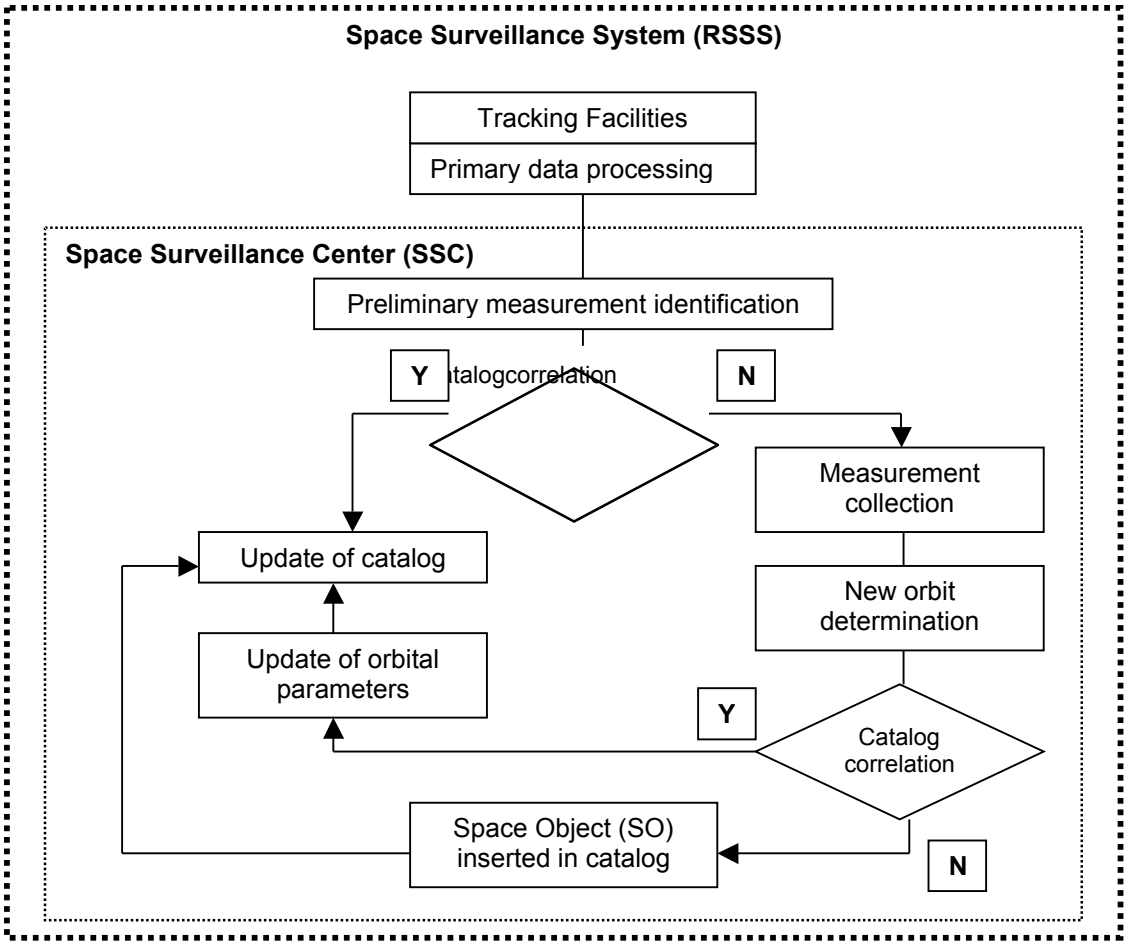

Fig. A-3: wire diagram depicting general element set processing scheme utilized by the Russian Space Surveillance Service (RSSS).

Also, several papers presented in the 1990s describe the sensors available to the RSSS. These are described below.

Sensor Site	Sensor Desig.	Latitude [deg]	Longitude [deg]	Azimuth Range [deg]	Sensor Type
Abustumani (Georgia)	ABA	42.00	43.00	0-360	Electro-Optical
Alma Ata (Kazakhstan)	ALM	43.00	77.00	0-360	Optical
Ashgabad (Turkmenia)	ASH	38.00	58.00	0-360	Electro-Optical
Balkhash (Kazakhstan)	BAL	45.00	74.00	30-330	BMEWS PAR
Dushanbe (Tadjikistan)	DUS	39.00	69.00	0-360	Optical
Irkutsk (Russia)	IR1	53.00	103.000	30-300	BMEWS PAR
Irkutsk (Russia)	IR2	52.00	100.000	0-360	Electro-Optical
Kiev (Ukraine)	KIE	50.00	30.00	0-360	Optical
Kourovka (Russia)	KOU	57.00	60.00	0-360	Optical
Mingechaur	MIN	41.00	48.00	105-215	BMEWS PAR

(Azerbaijan)					
Moscow “East” (Russia)	MO1	55.00	37.00	255-305	BMD PAR
Moscow “West” (Russia)	MO2	55.00	37.00	65-120	BMD PAR
Murmansk (Russia)	MUR	68.00	40.00	295-355	BMEWS PAR
Pechora (Russia)	PEC	65.00	57.00	300-55	BMEWS PAR
Riga (Latvia)	RIG	57.00	22.00	220-310	BMEWS PAR
Sevastopol (Ukraine)	SEV	44.00	33.00	140-260	BMEWS PAR
Simeiz (Ukraine)	SIM	44.00	34.00	0-360	Electro-Optical
Uzhgorod (Ukraine)	UZ1	48.00	23.00	165-285	BMEWS PAR
Uzhgorod (Ukraine)	UZ2	49.00	22.00	0-360	Optical
Yuhno-Sakhalins (Russia)	YUH	47.00	143.000	0-360	Optical
Zvenigorod (Russia)	ZVE	56.00	37.00	0-360	Optical

Herein, the acronym BMD indicates the Ballistic Missile Defense radar or radar system installed around Moscow. These sensors are presented in the next two figures so as to minimize the unavoidable clutter imposed by the relatively close geographical proximity of the RSSS sensors.

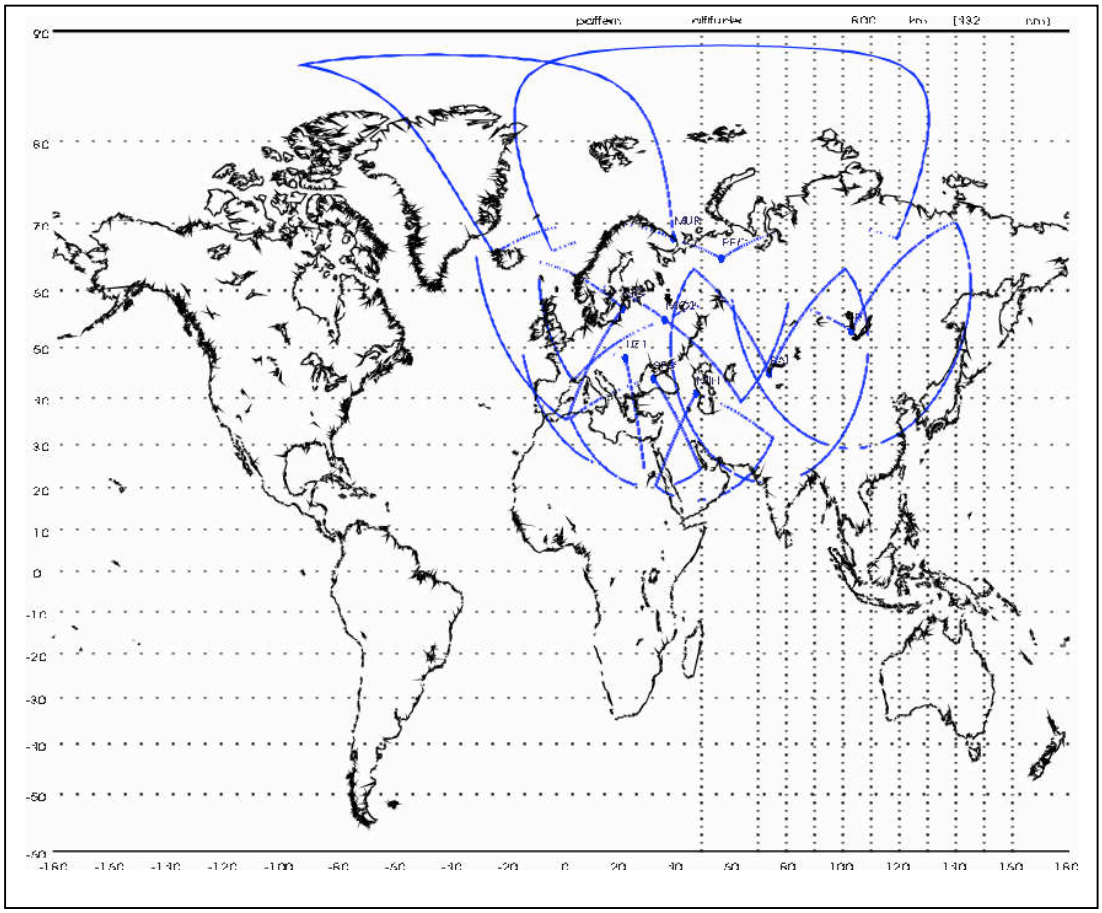

Fig. A-4: Russian RSSS radar assets.
Radiation patterns at 800 km altitude. Miller cylindrical projection.

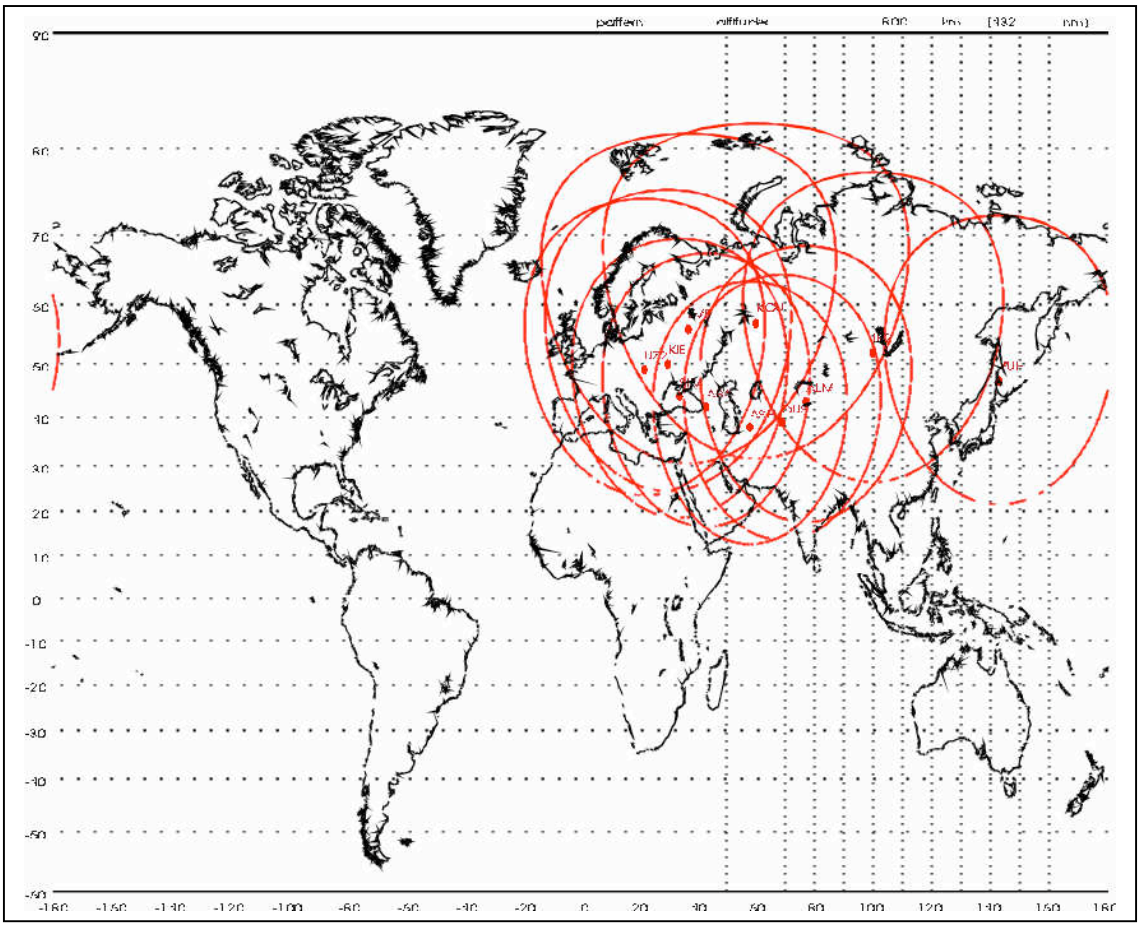

Fig. A-5: Russian RSSS optical sensor assets.
Pattern shown at 800 km altitude. Miller cylindrical projection.

Other space surveillance assets exist within the Former Soviet Union (FSU), *e.g.* the "Kobalt" mechanically-steered radar offered for charter or commercial use at the XVIII meeting of the Inter-Agency Debris coordination Committee (IADC). However, and in common with the sensors of the RSSS, the actual availability, serviceability, and current status of these sensors is unknown as of this writing. For example, more recent references (*e.g.* Whitmore, P.H., "Red Bear on the Prowl", Part 2, Quest **10**, no. 1 (2003): 54 ff.) indicate that the PAR sited at Riga, Latvia, may have been demolished in 1995, though an adjacent radar site may be operational.

A second caveat associated with the RSSS is associated with the geographic distribution of RSSS sensors. The Soviet fleet of Space Control ships has been long retired or converted to commercial maritime purposes; these were primarily

dedicated to space communications rather than space surveillance, in any case. As indicated by these figures, the RSSS is located within the confines of the FSU's borders. This places concomitantly greater restraints upon the RSSS as compared to the SSN tracking capability which, for example, manifests itself as consistently greater breaks in coverage of specific orbits as compared to the SSN. Thus, a high probability exists that (a) particular orbit classes, *e.g*. GEO and other low inclination or highly eccentric orbits are poorly tracked if at all, and (b) the RSSS catalog of RSOs is not as complete as the corresponding SCC catalog.

The RSSS collected (as of 1993) approximately 400 000 unique measurements per day, with approximately 10 000 orbits being updated. Stated accuracies of the RSSS tracking data are on the order of 4.5 km along track, 0.8 km "binormal component" (cross track), and 1.5 km in the radial direction. Current capabilities are unknown.

Availability of Data

As indicated previously, the cognizant Russian authorities have indicated that the RSSS, as well as other space surveillance-capable sensors such as the Kobalt radar, are "open for business" in terms of:

1. Informational support of space programs and experiments of concerned countries.
2. Coordinated operations in contingencies and notification of the concerned countries about dangerous situations in space and out of space.
3. Control of international agreements related to legal issues of using the near Earth space.
4. Informational provision for research on the upper atmosphere density variations.
5. Ecological monitoring of the near Earth space (space contamination control and analysis of its consequences).
6. Scientific provision of business cooperation mentioned above.

Russian RSSS data are not publicly available, but may be made available on a commercial data product/service. However, since these items are not publicly available, and given the caveats previously discussed, this discussion shall be limited only to a description of the data formats described by Russian representatives.

Data Format(s)

Several data formats are available from the RSSS. Internal data is believed to be maintained in state vector format. The format tabulated below (not guaranteed to be complete; an anomaly angular variable was not described) has been utilized in several international cooperative activities, such as the *Salyut*

7/*Cosmos 1686* reentry campaign. Finally, pseudo-TLEs have been provided in the course of international cooperative studies due to the near-universal nature of TLEs and the ability of user groups to process them in a standard manner.

ITEM	FORMAT/ VALUES	UNITS
International Designator	YY-NNN-N(NN)	(last two digits of year)(launch number within year)(numerical piece tag)
Number revolution	NNNNN	None
Epoch Time 1	DD.MM.YY	(day of month).(month).(last two digits of year)
Epoch Time 2/epoch of ascending node passage (beginning of revolution N)	HH.mm.ss.ss	(hours).(minutes).(fractional seconds)
Nodal period	NNNNN.NNNNN	minutes
Change in nodal period	± .NNNNN	Minutes/revolution
Inclination *i*	NNN.NNNN	Degrees
Right Ascension of Ascending Node □	NNN.NNNN	Degrees
Parameter of Laplace 1	.NNNNNNN	L = e·cos(□); unitless
Parameter of Laplace 2	.NNNNNNN	h = e·cos(□); unitless
Eccentricity e	.NNNNNNN	None
Argument of Perigee □	NNN.NNNN	Degrees
Ballistic coefficient	.NNNN±N	m^2/kg

Other Space Surveillance Assets

Two additional European assets have the proven capability to track and observe space objects (including debris). These are the French Navy ship *Le Monge* and the FGAN establishment's radar located in Germany.

Le Monge

The *Le Monge* is a French Navy laboratory, test, and instrumentation ship equipped with a meteorological and Laser Radar (LIDAR) station, a telemetry station, an optical station, and five radar stations. The radar stations are the *Stratus*, *Gascogne*, *Savoie*, and two *Armor* installations. These latter two radars can be used to observe debris, and in fact have supported collision avoidance activities for the SPOT satellites as early as 1997. The *Armor* radars are mechanically-tracked stabilized radars capable of scanning METOP altitudes above a minimum topocentric elevation of 20°.

Forschungsgesellschaft für Angewandte Naturwissenschaften e.V. (FGAN)

The FGAN Tracking and Imaging Radar (TIRA), located approximately 30 km south of Bonn, has a proven capability not only to track debris, but also to perform imaging of the target under scrutiny. In addition, the mechanically-

steered TIRA has participated in several international Beam Park Experiments (BPE) in association with other sensors worldwide. In a BPE, the pencil beam radar "stares" at a point in space and records objects traversing the beam; these experiments are useful for (a) providing the debris community validation of previous and continuing efforts with the LRIR/HAX radars and (b) providing a snapshot of the debris environment in low Earth orbit.

Orbital Data Provision

NASA Goddard Space Flight Center (GSFC) Orbital Information Group (OIG)

The NASA GSFC OIG is chartered to serve as the distribution center for USSTRATCOM-derived products. Currently, these data products are the TLEs and the NASA Satellite Situation Report (analogous to, though a subset of, the SCC catalog). The ability to download data products electronically is limited and is characterized by a user level. Base level users are limited in connect time, total number of TLEs downloaded, and the TLE sorts available. In order to minimize transmission time, and targeting or marketing to specific user communities (*e.g*. the amateur radio operators), TLEs available to a base level user are categorized by mission or altitude. The entire catalog is not available. To access the entire catalog, a user must have the so-called "superuser" status. This entitles the user to download the entire TLE catalog, comprising objects with catalog numbers in the 1-69999 range. Other user levels and/or Memoranda of Agreement (MOA) or Memoranda of Understanding (MOU) are required to access the catalog as well as the analyst catalog (*e.g*. the 80 000 series of TLEs). Unfortunately, the completeness of 80 000 series objects maintained by the OIG (relative to the total analyst set catalog maintained by the SCC) cannot be guaranteed.

USSTRATCOM

The USSTRATCOM has established procedures whereby Foreign Governments, Multinational Consortiums, Foreign Launch Agencies, or their US agents or representatives may request orbital information. Procedures differ slightly depending upon whether the entity has an existing MOA or MOU in place with either the USSTRATCOM SCC or NASA.

In the case in which the entity possesses an MOA or MOU with NASA, the data request is made directly to NASA GSFC under a 1994 MOU between NASA and USSTRATCOM SCC. NASA will forward the request to USSTRATCOM's Cheyenne Mountain Operations Center (CMOC), who will review the request and justifications and, if granted, supply the data to NASA GSFC for direct redistribution to the entity.

For the case in which the entity does not possess an MOA or MOU with NASA, the data request is made from the Foreign Government or entity to the United

State's Embassy in the requestor's country. The embassy forwards the request and justifications to the US Department of State (DOS). The DOS notifies the National Military Command Center (NMCC) Deputy Director of Operations (DDO), the CMOC, and NASA GSFC, and provides approval and release instructions. Data, if approved, will then be transmitted from either DOS or directly from NASA GSFC to the requestor.

Certain entities, such as the European Space Agency (ESA), have or will have MOAs in place with the USSTRATCOM SCC. The MOAs have, or will have, specific information channels identified by which data, and data content, shall be provided to an end user or user community.

Appendix C

US Government Guidelines

OBJECTIVE

1. CONTROL OF DEBRIS RELEASED DURING NORMAL OPERATIONS

Programs and projects will assess and limit the amount of debris released in a planned manner during normal operations.

MITIGATION STANDARD PRACTICES

1-1. *In all operational orbit regimes:* Spacecraft and upper stages should be designed to eliminate or minimize debris released during normal operations. Each instance of planned release of debris larger than 5 mm in any dimension that remains on orbit for more than 25 years should be evaluated and justified on the basis of cost effectiveness and mission requirements.

OBJECTIVE

2. MINIMIZING DEBRIS GENERATED BY ACCIDENTAL EXPLOSIONS

Programs and projects will assess and limit the probability of accidental explosion during and after completion of mission operations.

MITIGATION STANDARD PRACTICES

2-1. *Limiting the risk to other space systems from accidental explosions during mission operations:* In developing the design of a spacecraft or upper stage, each program, via failure mode and effects analyses or equivalent analyses, should demonstrate either that there is no credible failure mode for accidental explosion, or, if such credible failure modes exist, design or operational procedures will limit the probability of the occurrence of such failure modes.

2-2. *Limiting the risk to other space systems from accidental explosions after completion of mission operations:* All on-board sources of stored energy of a spacecraft or upper stage should be depleted or safed when they are no longer required for mission operations or postmission disposal. Depletion should occur as soon as such an operation does not pose an unacceptable risk to the payload. Propellant depletion burns and compressed gas releases should be designed to minimize the probability of subsequent accidental collision and to minimize the impact of a subsequent accidental explosion.

OBJECTIVE

3. SELECTION OF SAFE FLIGHT PROFILE AND OPERATIONAL CONFIGURATION

Programs and projects will assess and limit the probability of operating space systems becoming a source of debris by collisions with man-made objects or meteoroids.

MITIGATION STANDARD PRACTICES

3-1. *Collision with large objects during orbital lifetime:* In developing the design and mission profile for a spacecraft or upper stage, a program will estimate and limit the probability of collision with known objects during orbital lifetime.

3-2. *Collision with small debris during mission operations:* Spacecraft design will consider and, consistent with cost effectiveness, limit the probability that collisions with debris smaller than 1 cm diameter will cause loss of control to prevent post-mission disposal.

3-3. *Tether systems* will be uniquely analyzed for both intact and severed conditions.

OBJECTIVE

4. POSTMISSION DISPOSAL OF SPACE STRUCTURES

Programs and projects will plan for, consistent with mission requirements, cost effective disposal procedures for launch vehicle components, upper stages, spacecraft, and other payloads at the end of mission life to minimize impact on future space operations.

MITIGATION STANDARD PRACTICES

4-1. *Disposal for final mission orbits:* A spacecraft or upper stage may be disposed of by one of three methods:

a. Atmospheric reentry option: Leave the structure in an orbit in which, using conservative projections for solar activity, atmospheric drag will limit the lifetime to no longer than 25 years after completion of mission. If drag enhancement devices are to be used to reduce the orbit lifetime, it should be demonstrated that such devices will significantly reduce the area-time product of the system or will not cause spacecraft or large debris to fragment if a collision occurs while the system is decaying from orbit. If a space structure is to be disposed of by reentry into the Earth's atmosphere, the risk of human casualty will be less than 1 in 10,000.

b. Maneuvering to a storage orbit: At end of life the structure may be relocated to one of the following storage regimes:

I. Between LEO and MEO: Maneuver to an orbit with perigee altitude above 2000 km and apogee altitude below 19,700 km (500 km below semi-synchronous altitude

II. Between MEO and GEO: Maneuver to an orbit with perigee altitude above 20,700 km and apogee altitude below 35,300 km (approximately 500 km above semi-synchronous altitude and 500 km below synchronous altitude.)

III. Above GEO: Maneuver to an orbit with perigee altitude above 36,100 km (approximately 300 km above synchronous altitude)

IV. Heliocentric, Earth-escape: Maneuver to remove the structure from Earth orbit, into a heliocentric orbit.

Because of fuel gauging uncertainties near the end of mission, a program should use a maneuver strategy that reduces the risk of leaving the structure near an operational orbit regime.

c. Direct retrieval: Retrieve the structure and remove it from orbit as soon as practical after completion of mission.

4-2. *Tether systems* will be uniquely analyzed for both intact and severed conditions when performing trade-offs between alternative disposal strategies.